Title page.

Title:

Endothelin-1 suppresses insulin-stimulated Akt phosphorylation and glucose uptake via G protein-coupled receptor kinase 2 in skeletal muscle cells.

Short running title:

Mechanisms for ET-1-induced insulin resistance.

Author's names:

Takahiro Horinouchi, Akimasa Hoshi, Takuya Harada, Tsunaki Higa, Sarita Karki, Koji Terada, Tsunehito Higashi, Yosuke Mai, Prabha Nepal, Yuichi Mazaki, Soichi Miwa.

Author's address:

Department of Cellular Pharmacology, Hokkaido University Graduate School of Medicine, North 15, West 7, Kita-ku, Sapporo-City, Hokkaido 060-8638, Japan.

Corresponding author:

Takahiro Horinouchi, Ph.D.

Department of Cellular Pharmacology,

Hokkaido University Graduate School of Medicine,

North 15, West 7, Sapporo-City, Hokkaido 060-8638, Japan.

Tel: +81-11-706-6921

Fax: +81-11-706-7824

E-mail: horinouc@med.hokudai.ac.jp

Authorship contribution statement:

T Horinouchi, A Hoshi, T Harada, T Higa, S Karki, K Terada, T Higashi, Y Mai, P Nepal and Y Mazaki performed the research. T Horinouchi, A Hoshi and S Miwa designed the

research study. T Horinouchi, T Higa and S Miwa provided funding. T Horinouchi and S Miwa wrote the manuscript.

The number of characters in the Title: 146

The number of characters in the Short running title: 46

The number of words in the Abstract: 250

The number of words in the main body of the manuscript: 4,647

The number of words in the Discussion and conclusions: 1,158

The number of references: 45

The number of tables: 1

The number of figures: 10

The number of supplementary data: 5 (four Figures and one Movie)

Abstract page.

BACKGROUND AND PURPOSE

Endothelin-1 (ET-1) reduces insulin-stimulated glucose uptake in skeletal muscle, leading to the development of insulin resistance. The purpose of this study is to determine molecular mechanisms underlying negative regulation by ET-1 of insulin signaling.

EXPERIMENTAL APPROACH

Myoblasts of rat L6 skeletal muscle cell line were differentiated into myotubes. Western blotting was employed to analyze changes in the phosphorylation levels of Akt at threonine 308 (Thr^{308}) and serine 473 (Ser^{473}). Effect of ET-1 on insulin-stimulated glucose uptake was assessed with [^{3}H]-labelled 2-deoxy-D-glucose ([^{3}H]2-DG). C-terminus region of G protein-coupled receptor kinase 2 (GRK2-ct), a dominant negative GRK2, was overexpressed in L6 cells using adenovirus-mediated gene transfer. GRK2 expression was suppressed by transfection of siRNA.

KEY RESULTS

In L6 myotubes, insulin elicited sustained Akt phosphorylation at Thr^{308} and Ser^{473}, which was suppressed by ET-1. The inhibitory effects of ET-1 were counteracted by treatment with a selective ET type A receptor (ET_AR) antagonist and a G_q protein inhibitor, overexpression of GRK2-ct, and knockdown of GRK2. Insulin increased [^{3}H]2-DG uptake rate in a concentration-dependent manner. ET-1 noncompetitively antagonized insulin-stimulated [^{3}H]2-DG uptake. Blockade of ET_AR, overexpression of GRK2-ct and knockdown of GRK2 cancelled the ET-1-induced suppression of insulin-stimulated [^{3}H]2-DG uptake. In L6 myotubes overexpressing FLAG-GRK2, ET-1 facilitated the interaction of endogenous Akt with FLAG-GRK2.

CONCLUSIONS AND IMPLICATIONS

Activation of ET_AR with ET-1 suppresses insulin-induced Akt phosphorylation at Thr^{308} and

Ser^{473} and [^{3}H]2-DG uptake in a GRK2-dependent manner in skeletal muscle. These findings suggest that ET_AR and GRK2 are potential targets for insulin resistance.

Abbreviations

BSA, bovine serum albumin; DMEM, Dulbecco's modified Eagle's medium; ERK1/2, extracellular signal-regulated kinases 1/2; ET-1, endothelin-1; ET_AR, endothelin type A receptor; ET_BR, endothelin type B receptor; FCS, fetal calf serum; GLUT, glucose transporter; GPCR, G protein-coupled receptor; GRK2, G protein-coupled receptor kinase 2; GRK2-ct, C-terminus region of G protein-coupled receptor kinase 2; GSV, glucose transporter storage vesicle; [^{3}H]2-DG, [1,2-^{3}H(N)]-2-deoxy-D-glucose; HRP, horseradish peroxidase; HS, horse serum; IR, insulin receptor; IRS, insulin receptor substrate; PDK1, phosphoinositide-dependent kinase 1; PI3K, phosphatidylinositol 3-kinase; PTX, pertussis toxin; qRT-PCR, quantitative reverse transcription-polymerase chain reaction; Rab-GTPase, Rab guanosine triphosphatase; siRNA, short interfering RNA.

Introduction

Endothelin-1 (ET-1) is a potent vasoconstrictor and pro-inflammatory peptide (Yanagisawa *et al.*, 1988), that has been implicated in the pathophysiology of various diseases, including diabetes mellitus (Pernow *et al.*, 2012), systemic and pulmonary hypertension (Rodríguez-Pascual *et al.*, 2011), and atherosclerosis (Pernow *et al.*, 2012). It is reported that ET-1 levels in the plasma are elevated in patients with these diseases (Ferri *et al.*, 1995; Lerman *et al.*, 1991; Takahashi *et al.*, 1990; Touyz *et al.*, 2003). Excessive production of ET-1 causes a prolonged vasoconstriction mediated mainly through ET type A receptor (ET_AR) (Horinouchi *et al.*, 2013), endothelial dysfunction resulting from downregulation of ET_BR (Rubin, 2012), and insulin resistance (Shemyakin *et al.*, 2011; Usui *et al.*, 2005).

Insulin resistance is a condition where the sensitivity to insulin of the cells expressing insulin receptor (IR) is decreased because of a functional disturbance of insulin-mediated intracellular signaling. The most important tissue responsible for the insulin's action of decreasing blood glucose levels is skeletal muscle which accounts for approximately 70% of total glucose uptake in healthy subjects (DeFronzo, 1988). Accordingly, disturbance of insulin-stimulated glucose uptake into skeletal muscle is mainly responsible for elevated blood glucose levels in patients with type 2 diabetes (DeFronzo, 1988), where there is no significant change in glucose transporter 4 (GLUT4) protein levels (Schalin-Jäntti et al., 1994).

Insulin increases glucose uptake rate in skeletal muscle cells through facilitating translocation of GLUT4 from intracellular GLUT storage vesicle (GSV) to the plasma membrane (Leto *et al.*, 2012). Activation of IR induces phosphorylation of IR substrate (IRS) proteins, resulting in the recruitment and activation of phosphatidylinositol 3-kinase (PI3K) (Leto *et al.*, 2012). PI3K converts phosphatidylinositol-4,5-diphosphate to phosphatidylinositol-3,4,5-trisphosphate which is involved in the recruitment of phosphoinositide-dependent kinase 1 (PDK1) and Akt (Leto *et al.*, 2012; Shisheva, 2008). Akt translocated to the plasma membrane is activated by phosphorylation at threonine 308 (Thr^{308}) by PDK1 and at serine 473 (Ser^{473}) by mammalian target of rapamycin complex 2 (Laplante *et al.*, 2012; Leto *et al.*, 2012; Sarbassov *et al.*, 2005). Activated Akt facilitates

the translocation of GLUT4 to the plasma membrane by phosphorylation and subsequent inactivation of the Rab guanosine triphosphatase (GTPase)-activating protein, AS160 (Leto *et al.*, 2012). The decreased Rab-GTPase activity increases the ratio of the GTP-bound form (active form) of Rab to the GDP-bound form (inactive form), leading to facilitation of GLUT4 translocation and cell membrane fusion (Leto *et al.*, 2012). These data implicate that Akt activation is essential for insulin-stimulated glucose uptake via GLUT4 in skeletal muscle.

Several studies have suggested that ET-1 induces insulin resistance through a direct action on skeletal muscle, but not through a reduced insulin delivery to the skeletal muscle resulting from vasoconstriction. That is, in healthy subjects, administration of exogenous ET-1 reduces insulin-stimulated glucose uptake in skeletal muscle without decreasing skeletal muscle blood flow (Ottosson-Seeberger *et al.*, 1997). In addition, prolonged treatment of primary culture of human skeletal muscle cells with ET-1 impairs insulin-stimulated Akt phosphorylation and glucose uptake (Shemyakin *et al.*, 2011). However, the signaling pathways underlying the inhibitory effects of ET-1 on the insulin-induced facilitation of Akt phosphorylation and glucose uptake in skeletal muscle cells are unknown.

Growing evidence shows that G protein-coupled receptor (GPCR) kinase 2 (GRK2), a ubiquitous Ser/Thr protein kinase, can function as a negative regulator of insulin signaling in phosphorylation-independent manner, although it was originally identified as a kinase which specifically phosphorylates and desensitizes agonist-stimulated GPCRs (Evron *et al.*, 2012). Several lines of evidence demonstrate that GRK2 binds to numerous signaling molecules including Akt (Liu *et al.*, 2005) and $G_{\beta\gamma}$ subunits (Evron *et al.*, 2012). A direct interaction of GRK2 with Akt impairs Akt activation, causing negative regulation of Akt signaling (Liu *et al.*, 2005). Binding of GRK2 to $G_{\beta\gamma}$ subunits is essential for translocation of GRK2 to the plasma membrane (Evron *et al.*, 2012). These data encouraged us to assume that activation of ETRs in skeletal muscle cells induces insulin resistance through inhibition of Akt signaling: namely, activation of ETRs promotes dissociation of receptor-coupled G protein into its subunits, G_{α} and $G_{\beta\gamma}$; the increase in the local concentration of $G_{\beta\gamma}$ subunit in turn recruits GRK2 to the plasma membrane, leading to the augmented interaction of GRK2 with

Akt at the plasma membrane and the resulting inhibition of Akt signaling.

The purpose of this study was to determine molecular mechanisms underlying negative regulation by ET-1 of insulin signaling in rat L6 myotubes with special attention to possible involvement of GRK2. Since both protein contents of GLUT4 and insulin-stimulated glucose uptake via GLUT4 were increased during myogenesis in L6 cells (Mitsumoto *et al.*, 1992), L6 myoblasts were highly differentiated into myotubes with a modified method to estimate insulin-stimulated glucose uptake.

METHODS

Materials

YM-254890 was kindly provided by Astellas Pharma Inc. (Tokyo, Japan). The following drugs and reagents were used in the present study: synthetic human ET-1, BQ-123 [cyclo(D-trp-D-asp-L-pro-D-val-L-leu)], BQ-788 (N-cis-2,6-dimethyl-piperidinocarbonyl-L-γ-methylleucyl-D-1-methoxycarbonyltryptophanyl-D-norleucine) (Peptide Institute, Osaka, Japan); human insulin (Cell Science and Technology Institute, Inc., Miyagi, Japan); bovine serum albumin (BSA), Hoechst 33342 (Sigma-Aldrich Co., St. Louis, MO, U.S.A.); LY294002 [2-(4-morpholinyl)-8-phenyl-4H-1-benzopyran-4-one], pertussis toxin (PTX) (Calbiochem, San Diego, CA, U.S.A.); [1,2-^{3}H(N)]-2-deoxy-D-glucose ([^{3}H]2-DG; specific activity: 8.0 Ci mmol^{-1}, 1.0 mCi ml^{-1} in aqueous solution, PerkinElmer, Inc., Boston, MA, U.S.A.); fetal calf serum (FCS), horse serum (HS), D-glucose- and sodium pyruvate-free Dulbecco's modified Eagle's medium (DMEM), EDTA-free, protease inhibitor cocktail (Thermo Fisher Scientific Inc., Waltham, MA, U.S.A.); low-glucose (5.5 mM) DMEM (Wako Pure Chemical Industries, Ltd., Osaka, Japan); GSK2126458 [2,4-difluoro-N-(2-methoxy-5-(4-(pyridazin-4-yl)quinolin-6-yl)pyridin-3-yl)benzenesulfonamide] (Selleck Chemicals, Houston, TX, U.S.A.); NF449 (4,4',4",4"'-[carbonylbis(imino-5,1,3-benzenetriyl-bis(carbonylimino))]tetrakis-1,3-benzenedisulfonic acid, octasodium salt) (Tocris Bioscience, Moorend Farm Avenue, Bristol, U.K.); ON-TARGETplus Rat Adrbk1 (25238) siRNA - SMARTpool (L-090990-02-0005), ON-TARGETplus Non-targeting Pool (D-001810-10-05) (GE Healthcare Dharmacon Inc., Lafayette, CO, U.S.A.); Lipofectamine RNAiMAX Transfection Reagent, Opti-MEM I Reduced Serum Medium (Thermo Fisher Scientific Inc.). Primary antibodies for phospho-Akt (Thr^{308}), phospho-Akt (Ser^{473}), total Akt (pan), phospho-extracellular signal-regulated kinases 1/2 (phospho-ERK1/2) (Thr^{202}/Tyr^{204}), total ERK1/2, and IRS-1, and a secondary horseradish peroxidase (HRP)-conjugated anti-rabbit IgG antibody were obtained from Cell Signaling Technology Inc. (Beverly, MA, U.S.A.). Primary antibodies for FLAG peptide, HRP-conjugated FLAG peptide (HRP-FLAG) and green fluorescent protein (GFP)

were obtained from Sigma-Aldrich, Medical and Biological Laboratories Co., Ltd. (Aichi, Japan) and Clontech Laboratories, Inc. (Mountain View, CA, U.S.A.), respectively. GRK2 antibody (C-15) and normal mouse IgG were obtained from Santa Cruz Biotechnology, Inc. (Dallas, TX, U.S.A.). Clean-Blot IP Detection Reagent HRP was obtained from Thermo Fisher Scientific Inc. The other regents used were of analytical grade.

Construction of retrovirus vector

The pcDNA3 mammalian expression vector encoding FLAG-tagged GRK2 (FLAG-GRK2) was generously provided by Dr. Hitoshi Kurose (Kyusyu University, Fukuoka, Japan). The vector was digested with two restriction enzymes (BamHI and NotI) simultaneously to obtain the insert cDNA of FLAG-GRK2. The cDNA fragment was ligated into the BamHI/NotI-treated pMXrmv5 retrovirus vector to yield the pMXrmv5 vectors encoding FLAG-GRK2.

Cell culture

Rat L6 skeletal muscle cell line was obtained from the Health Science Research Resources Bank (Osaka, Japan), and cultured in low-glucose DMEM supplemented with 5% (v v^{-1}) FCS, penicillin (100 units mL^{-1}), and streptomycin (100 μg mL^{-1}) at 37°C in humidified air with 5% CO_2. For differentiation of myoblasts into myotubes, myoblasts were seeded into 6-well plates at a density of approximately 10^6 cells per well and cultured in low-glucose DMEM supplemented with 5% FCS for 2 days. To induct differentiation, the cells were maintained in low-glucose DMEM supplemented with 2% HS and 10 μg mL^{-1} human insulin for 7 days with medium change every two days (Figure 1A). For Western blot analysis and [^{3}H]2-DG uptake assay, the differentiated myotubes (Day 7) were serum-starved in low-glucose DMEM for 2 or 3 days with daily medium change prior to performing the examination (unless indicated otherwise).

Stable expression of FLAG-GRK2 in L6 cells

To generate L6 cells stably expressing FLAG-GRK2, the gene was introduced into L6

myoblasts by retroviral gene transfer as described previously (Horinouchi *et al.*, 2012).

Adenovirus infection

Recombinant adenoviruses encoding GFP and the carboxyl terminal region of GRK2 (GRK2-ct) were kindly provided by Dr. Hitoshi Kurose (Kyusyu University). L6 myotubes (Day 7) maintained in 6-well plates were infected by recombinant adenoviruses encoding GFP or GRK2-ct for 2 h. After infection, the cells were cultured in low-glucose DMEM containing 2% HS for 12 h. Subsequently, L6 myotubes were cultured in serum-free, low-glucose DMEM for 2 days for Western blot analysis or 3 days for [^{3}H]2-DG uptake assay.

Transfection of siRNA

Control and GRK2 siRNAs were transfected into L6 myotubes (Day 6) maintained in 6-well plates using Lipofectamine RNAiMAX Transfection Reagent according to the manufacturer's protocol with minor modifications. Briefly, 40 pmol of siRNA was diluted in 0.5 mL of Opti-MEM I without serum. 7.5 μL of Lipofectamine RNAiMAX Transfection Reagent was diluted in the diluted siRNA solution, and the mixture was incubated at room temperature for 20 min. Cell culture medium was removed from wells of 6-well plates, and the mixture of siRNA and Lipofectamine RNAiMAX Transfection Reagent was added to each well. Then, 0.5 mL of low-glucose DMEM containing 0.5% FCS was added to the well without removing the transfection mixture, and the cells were incubated for 72 h. During 72 h incubation, 0.5 mL of low-glucose DMEM was added to each well every 24 h without removing the transfection mixture. For Western blot analysis and [^{3}H]2-DG uptake assay, the cells were serum-starved in low-glucose DMEM for 24 h prior to performing the examination.

Visualization of cell nuclei and imaging of spontaneously contracting myotubes

L6 myoblasts (Day 0) and myotubes (Days 7 and 9) were incubated with a DNA-specific fluorescent dye, Hoechst 33342 (1 μg mL^{-1}), for 30 min in culture medium at

37°C in humidified air with 5% CO_2. The fluorescent images for Hoechst 33342 and the phase contrast images were obtained using a fluorescence microscopy (IX-71, Olympus Corp., Tokyo, Japan) equipped with × 20 objective lens (LUCPLFLN, NA = 0.45, Olympus).

Measurement of mRNA expression levels for MyoD, myogenin, and 18S rRNA by quantitative reverse transcription-polymerase chain reaction (qRT-PCR)

Total RNA of L6 cells was extracted at indicated days (Figure 1CD) and purified by using total RNA purification kit (RNeasy Mini Kit, QIAGEN, Tokyo, Japan) following the instructions of the manufacturer. qRT-PCR was performed by using both SuperScript III First-Strand Synthesis System (Thermo Fisher Scientific Inc.) for RT and FastStart Essential DNA Green Master kit (Roche Diagnostics GmbH, Mannheim, Germany) with gene-specific primers for qPCR (Table 1). Synthesized cDNA was heated for 10 min at 95°C, then amplified by 45 cycles (95°C for 10 s, 60°C for 10 s and 72°C for 15 s) using a programmable thermal cycler (LightCycler Nano; Roche Diagnostics GmbH). The PCR products were confirmed by a single band on electrophoresis and by the single melting temperature. The 18S rRNA gene was used as an internal control for normalization of the data. Expression levels of mRNAs for MyoD and myogenin were represented as a ratio to 18S rRNA.

Western blot analysis

Western blot analysis was carried out as described previously (Harada *et al.*, 2014). The primary antibodies [phospho-Akt (Thr^{308}), phospho-Akt (Ser^{473}), total Akt (pan), phospho-ERK1/2, total-ERK1/2, and IRS-1] bound to proteins on membranes were detected with a secondary HRP-conjugated anti-rabbit IgG antibody and Pierce Western Blotting Substrate (Thermo Fisher Scientific Inc.). The blots were exposed to Amersham Hyperfilm ECL (GE Healthcare Ltd., Little Chalfont, Buckinghamshire, U.K.). Optical density on the film was analyzed with National Institutes of Health Image J1.37 software. The phosphorylation levels of Akt at Thr^{308} and Ser^{473} were routinely expressed as the ratio of phosphorylated Akt to total Akt. Akt phosphorylation responses were normalized to the

level of insulin-stimulated Akt phosphorylation in L6 myotubes without treatment with ET-1, vehicle, antagonist, inhibitor, adenovirus, or siRNA.

Coimmunoprecipitation assay

Coimmunoprecipitation experiment and subsequent Western blot analysis were carried out as described previously (Horinouchi *et al.*, 2012). The primary antibody [total Akt (pan) and IRS-1] bound to proteins on membranes was detected with Clean-Blot IP Detection Reagent HRP for immunoprecipitated samples or a secondary HRP-conjugated anti-rabbit IgG antibody for whole cell lysates. The Clean-Blot reagent and HRP-conjugated antibody were detected with ImmunoStar LD (Wako Pure Chemical Industries, Ltd.) and Pierce Western Blotting Substrate (Thermo Fisher Scientific Inc.), respectively. The membranes were then stripped with stripping buffer [62.5 mM Tris-HCl (pH 7.0), 2% sodium dodecyl sulfate, 1% 2-mercaptoethanol] for 1 h at 50°C and reprobed with an anti-FLAG HRP antibody. The blots were exposed to Amersham Hyperfilm ECL (GE Healthcare Ltd.). The amounts of immunoprecipitated proteins were analyzed with National Institutes of Health Image J1.37 software.

[^{3}H]2-DG uptake assay

L6 myotubes (Day 7) maintained in 6-well plates were serum-starved in low-glucose DMEM for 3 days (unless indicated otherwise) prior to performing [^{3}H]2-DG uptake assay. The cells were incubated in serum-free DMEM supplemented with 1.0 mM D-glucose and 1.0 mM sodium pyruvate (assay medium) for 30 min before each experiment. To estimate insulin-stimulated [^{3}H]2-DG uptake, the cells were treated with insulin and 100 nM [^{3}H]2-DG in serum-free assay medium. [^{3}H]2-DG uptake was terminated by rapid washing three times with 3 mL of phosphate-buffered saline (37°C) containing 20.0 mM D-glucose. For quantitation of [^{3}H]2-DG uptake, the cells were collected with 1.0 mL of 0.5 M NaOH (60°C), and completely digested with shaking at 150 rpm for 60 min at 60°C. The radioactivity in the lysate was counted in a liquid scintillation counter (LC-3500; Aloka, Tokyo, Japan) using a scintillation fluid (Clear-sol II; Nacalai Tesque Inc., Kyoto, Japan).

The protein content in the lysate was determined with the method of Bradford (1976) using BSA as standard.

Data Analysis

The results are presented as means ± S.E.M. where *n* refers to the number of experiments. The significance of the difference between mean values was evaluated with GraphPad Prism (version 3.00, GraphPad Software Inc., San Diego, CA, U.S.A.) by unpaired *t*-test or one-way analysis of variance followed by Tukey's multiple comparison test. A *P* value less than 0.05 was considered to indicate significant differences.

Results

Differentiation of mononucleated myoblasts into contractile, multinucleated myotubes

Figure 1B shows that mononucleated myoblasts (Day 0) are differentiated into multinucleated myotubes (Day 7) during culture in the differentiation medium. Some of myotubes (Day 7) possessed the ability to spontaneously constrict (Supplementary Movie S1). The myotubes (Day 7) were resistant to serum starvation for at least 3 days (Figure 1B, Day 9 after serum starvation for 2 days). qRT-PCR analysis has demonstrated that mRNA expression levels for differentiation marker genes, MyoD and myogenin (Bentzinger *et al.*, 2012), are increased during differentiation for 9 days with a different time course (Figure 1CD). The maximal mRNA expression level of MyoD was observed at Day 5 and was maintained for at least 4 days (Figure 1C). On the other hand, the mRNA expression level of myogenin was increased with time and reached its maximum at Day 9 (Figure 1D).

As shown in Supplementary Figure S1, the expression level of mRNA for ET_AR was slightly but significantly decreased after differentiation. On the other hand, mRNA expression levels of GRK2 and GLUT4 were increased after differentiation. There was no statistically significant difference in mRNA expression levels of G_q protein, G_{11} protein, IR and Akt2 between Day 0 and Day 7.

Characterization of insulin-induced Akt phosphorylation in L6 myotubes

Treatment of L6 myotubes with insulin at concentrations ranging from 1 nM to 3 μM for 5 min elicited phosphorylation of Akt at Thr^{308} and Ser^{473} in a concentration-dependent manner with pEC_{50} values of 7.59 ± 0.08 for Thr^{308} and 7.63 ± 0.08 for Ser^{473} (n = 6 for each) (Figure 2A). There was no statistically significant difference in the pEC_{50} values for phosphorylation of Thr^{308} and Ser^{473}. The phosphorylation of Akt induced by 300 nM insulin was increased rapidly after insulin stimulation, reached the maximal level at around 5 min and was kept at that level up to 15 min: the level of phosphorylation declined slightly at 30 min and remained constant up to 60 min (Figure 2B). The Akt phosphorylation at Thr^{308} and Ser^{473} in response to stimulation with 300 nM insulin for 5 min was significantly inhibited by PI3K inhibitors, 10 nM GSK2126458 (Knight *et al.*, 2010) and 50 μM

LY294002 (Shepherd *et al.*, 1997) (Figure 2CD).

Effects of ET-1 on insulin-induced Akt phosphorylation in L6 myotubes

In the absence of insulin stimulation, treatment with 30 nM ET-1 for the corresponding times had no significant effect on basal levels of Akt phosphorylation (Supplementary Figure S2). Akt phosphorylation at Thr^{308} and Ser^{473} induced by 100 nM insulin stimulation for 60 min was inhibited by treatment with 30 nM ET-1, and the extent of the inhibition became larger with time of ET-1 treatment: the maximal inhibition of around 50% was observed following ET-1 treatment for 10 - 15 min (Figure 3).

Molecular mechanisms for ET-1-induced inhibition of insulin-stimulated Akt phosphorylation in L6 myotubes

In the presence of 0.1% DMSO (as a vehicle), treatment with ET-1 for 2 min and 5 min inhibited phosphorylation of Akt at Thr^{308} and Ser^{473} induced by treatment with 100 nM insulin for 60 min (Figure 4). Notably, the inhibitory effects of ET-1 were counteracted by treatment with 1 μM BQ-123 (a selective ET_AR antagonist) and 300 nM YM-254890 (a selective G_q protein inhibitor). However, 1 μM BQ-788 (a selective ET_BR antagonist), 200 ng mL^{-1} PTX (a selective G_i protein inhibitor) and 100 μM NF449 (a G_s protein inhibitor) had no effect on the ET-1-induced inhibition of insulin-stimulated Akt phosphorylation.

Involvement of GRK2 in the ET-1-induced inhibition of insulin-stimulated Akt phosphorylation in L6 myotubes

As shown in Figure 5, overexpression of GFP as a control or GRK2-ct, a dominant negative construct lacking the N-terminal kinase domain (Koch *et al.*, 1994; Kurose *et al.*, 1999), had no effect on the insulin-stimulated Akt phosphorylation at Thr^{308} and Ser^{473}. In L6 myotubes overexpressing GFP, treatment with ET-1 for 2 min and 5 min decreased the phosphorylation levels of Akt at Thr^{308} and Ser^{473} induced by treatment with 100 nM insulin for 60 min (Figure 5). The inhibition by ET-1 of insulin-stimulated Akt phosphorylation was cancelled by overexpression of GRK2-ct.

In L6 myotubes transfected with non-targeting siRNA (control siRNA), ET-1 inhibited the insulin-stimulated Akt phosphorylation at Thr^{308} and Ser^{473} (Figure 6). On the other hand, GRK2 knockdown by GRK2 siRNA abrogated the ET-1-induced inhibition of insulin-stimulated Akt phosphorylation.

Effects of insulin on [^{3}H]2-DG uptake in L6 myotubes

Insulin increased the rate of [^{3}H]2-DG uptake in myotubes (Figure 7B), whereas it failed to facilitate [^{3}H]2-DG uptake in L6 myoblasts (data not shown), indicating that the insulin-stimulated glucose uptake is a myotube-specific response. In the absence of insulin, the basal uptake rate of [^{3}H]2-DG was 338.8 ± 13.2 dpm μg^{-1} h^{-1} (n = 12) (Figure 7B). Treatment of L6 myotubes with 100 nM insulin for 2 h increased [^{3}H]2-DG uptake rate (508.0 ± 20.3 dpm μg^{-1} h^{-1}, n = 12), and the insulin-stimulated [^{3}H]2-DG uptake was inhibited by PI3K inhibitors, 10 nM GSK2126458 and 50 μM LY294002, both of which did not affect the basal [^{3}H]2-DG uptake rate (Figure 7B). Insulin (3 - 300 nM) increased [^{3}H]2-DG uptake rate in a concentration-dependent manner: the pEC_{50} value was 8.08 ± 0.11 and the maximal response induced by 100 nM insulin was 154.6 ± 5.2 % of the basal uptake rate (n = 12) (Figure 7C). 30 nM ET-1 noncompetitively antagonized insulin-stimulated [^{3}H]2-DG uptake (pEC_{50} value: 7.86 ± 0.29, n = 6) without statistically significant change in the pEC_{50} values calculated from each concentration-response curve.

Molecular mechanisms for ET-1-induced inhibition of insulin-stimulated [^{3}H]2-DG uptake in L6 myotubes

In L6 myotubes, treatment with ET-1 or BQ-123, overexpression of GRK2-ct and transfection of GRK2 siRNA had no effect on the basal [^{3}H]2-DG uptake rate in the absence of insulin stimulation (data not shown). 30 nM ET-1 inhibited the insulin-stimulated [^{3}H]2-DG uptake from 159.2 ± 7.3% to 135.7 ± 4.5% (n = 8) (Figure 8A). The inhibitory effect of ET-1 was cancelled by pretreatment with 1 μM BQ-123 (Figure 8A). Notably, the ET-1-induced inhibition of insulin-stimulated [^{3}H]2-DG uptake was significantly counteracted by either overexpression of GRK2-ct (n = 8) (Figure 8B) or GRK2 knockdown

(n = 6) (Figure 8C).

Augmentation by ET-1 stimulation of interaction of Akt with GRK2 in L6 myotubes

A coimmunoprecipitation assay has revealed that endogenous Akt is nonspecifically immunoprecipitated with mouse normal IgG (control IgG) under resting condition (Figure 9A). Treatment of myotubes with 30 nM ET-1 for 5 min or 10 min resulted in approximately 2.5-fold increase in the amount of Akt protein which was coimmunoprecipitated with FLAG-GRK2, as compared to the value of basal interaction without ET-1 stimulation (Figure 9B). Unexpectedly, insulin stimulation alone augmented the interaction of Akt with FLAG-GRK2 in the absence of ET-1 stimulation, and the augmentation by insulin of the interaction was markedly attenuated by ET-1 stimulation for 10 min (Figure 9C). Accordingly, there was a discrepancy in the effect of ET-1 on the insulin-stimulated Akt phosphorylation between FLAG-GRK2-negative and positive cells: that is, ET-1 inhibited the insulin-stimulated Akt phosphorylation in L6 myotubes not overexpressing FLAG-GRK2 (Figure 3), whereas the inhibitory effect of ET-1 was not observed in the cells overexpressing FLAG-GRK2 (data not shown).

Discussion

In the present study, we have investigated the mechanism for ET-1-induced insulin resistance using the L6 myotubes. We demonstrate that ET-1 inhibits insulin-stimulated Akt phosphorylation and glucose uptake in L6 myotubes and that the ET_AR-G_q protein pathway and GRK2 are involved in the inhibitory effects of ET-1 (Figure 10).

The L6 skeletal muscle cell line is widely employed as a model for studying glucose transport and myogenesis. L6 myoblasts have the potential ability to spontaneously differentiate into myotubes (Nevzorova *et al.*, 2002). To differentiate L6 myoblasts into myotubes, we used differentiation medium containing both 2% HS and 10 μg mL^{-1} insulin, although many investigators employed the medium supplemented with either one of 2% FCS (Nevzorova *et al.*, 2002), 2% HS (Ruest *et al.*, 2002) or 10 μg mL^{-1} insulin (Jin *et al.*, 1991). The criteria for differentiation of myoblasts into myotube are as follows: (i) multinucleation, (ii) spontaneous contraction, (iii) an increase in expression level of transcription factors such as MyoD and myogenin, and (iv) an increase in expression level of GLUT4 (Bentzinger *et al.*, 2012; Mitsumoto *et al.*, 1991; Mitsumoto *et al.*, 1992; Öberg *et al.*, 2011). The L6 myotubes differentiated in differentiation medium containing both 2% HS and 10 μg mL^{-1} insulin fulfill the above criteria, indicating that these myotubes are highly differentiated (mature) skeletal muscle cells.

In the differentiated L6 myotubes, insulin stimulated PI3K-dependent Akt phosphorylation (Figure 2CD) and [^{3}H]2-DG uptake (Figure 7B) as an index of glucose uptake. These results are consistent with previous studies showing that PI3K inhibitors, wortmannin and LY 294002, inhibit insulin-stimulated Akt phosphorylation and glucose uptake in skeletal muscle cells (Nevzorova *et al.*, 2002; Shepherd *et al.*, 1997; Tsakiridis *et al.*, 1995), and indicate that L6 myotubes used in the present study possess functional IR and IR-stimulated intracellular signaling pathway leading to GLUT4. Indeed, expression of IR, IRS-1, Akt and GLUT4 in L6 myotubes was detected by RT-PCR (Supplementary Figure S1) or Western blot analysis (Supplementary Figure S3).

Several studies have demonstrated that in adipocytes, insulin stimulates GLUT4-mediated glucose uptake through IRS-independent pathway in addition to the

classical IRS-dependent pathway (Imamura *et al.*, 1999; Usui *et al.*, 2005; Usui *et al.*, 2003). That is, in adipocytes, insulin stimulation can activate a $G_{\alpha q}$ protein independently of IRS, and the activated $G_{\alpha q}$ subunit stimulates GLUT4-mediated glucose uptake through activation of Cdc42 and PI3K (Imamura *et al.*, 1999; Usui *et al.*, 2005; Usui *et al.*, 2003). This raises the possibility that activation of G_q protein is involved in the insulin-stimulated, PI3K-dependent Akt phosphorylation in L6 myotubes. However, this possibility was ruled out on the basis of insensitivity to YM-254890, a selective G_q protein inhibitor (Supplementary Figure S4).

The present study has shown that in L6 myotubes, ET-1 inhibits insulin-stimulated Akt phosphorylation (Figure 3) and [^{3}H]2-DG uptake (Figure 7), as reported previously (Shemyakin *et al.*, 2011). In our recent report, we have shown that in L6 myoblasts, both ET_AR and ET_BR are expressed at mRNA level (Harada *et al.*, 2014). ET_AR can couple with G_q and G_s proteins, while ET_BR can couple to G_q and G_i proteins (Alexander *et al.*, 2011). Based on the sensitivity to several types of antagonists and inhibitors (Figure 4), the ET-1-induced inhibition of the insulin-stimulated Akt phosphorylation and [^{3}H]2-DG uptake is considered to be mediated through the ET_AR-G_q protein pathway. The dominant role of the ET_AR-G_q protein pathway in L6 myotubes is consistent with that in the ET-1-induced ERK1/2 phosphorylation and Ca^{2+} influx in L6 myoblasts, as shown in our recent report (Harada *et al.*, 2014). These findings support clinical evidence that selective ET_AR blockade improves insulin-mediated glucose uptake in obese subjects (Lteif *et al.*, 2007).

The present study has demonstrated that the ET-1-mediated inhibition of insulin's action results from the augmented interaction of GRK2 with Akt and the subsequent inhibition of insulin-stimulated Akt phosphorylation. This conclusion is based on (i) attenuation of the ET-1-mediated inhibition of insulin-stimulated Akt phosphorylation and glucose uptake following overexpression of GRK2-ct (Figures 5 and 8) or GRK2 knockdown by siRNA (Figures 6 and 8) and (ii) augmentation by ET-1 of association between Akt and GRK2. GRK2 consists of an N-terminus kinase domain and a C-terminus containing the pleckstrin homology domain which is involved in the binding of GRK2 to several signaling molecules such as $G_{\beta\gamma}$ subunits and Akt (Evron *et al.*, 2012; Liu *et al.*, 2005). Because GRK2-ct lacks

the N-terminus kinase domain but it retains the ability to bind to other molecules, it can function as a dominant-negative form of GRK2 (Koch *et al.*, 1994; Nishida *et al.*, 2000), which interferes with the interaction between GRK2 and its binding partner molecules. In fact, GRK2 is reported to interact with Akt via its C-terminal region in rat endothelial cells (functionally disturbed by a pathological process such as diabetes mellitus) to reduce Akt phosphorylation (Liu *et al.*, 2005). Taken together, the present findings strongly indicate that GRK2 inhibits insulin-stimulated Akt phosphorylation, by interacting with Akt via its C-terminal region.

Unexpectedly, in L6 myotubes overexpressing FLAG-GRK2, insulin augmented the binding of Akt to FLAG-GRK2, and the augmentation was inhibited by ET-1 treatment for 10 min. The inhibitory effect of ET-1 on the insulin-stimulated interaction of overexpressed FLAG-GRK2 with Akt might be due to that βγ subunits released from $G_{\alpha q}$ protein upon activation of ET_AR compete with Akt for C-terminus region of FLAG-GRK2. The insulin-stimulated interaction of FLAG-GRK2 with Akt might inhibit phosphorylation of Akt like the ET-1-stimulated interaction, resulting in loss of ET-1-induced, GRK2-mediated inhibition of insulin-stimulated Akt phosphorylation. Further studies will be required to clarify the mechanism for insulin-stimulated interaction of FLAG-GRK2 with Akt.

In addition to Akt, IRS-1 is a potential target for ET-1-induced, GRK2-mediated inhibition of insulin-stimulated glucose uptake (Usui *et al.*, 2005; Usui *et al.*, 2004). IRS-1 is one of the major substrates of the IR kinase, and it contains multiple Ser/Thr phosphorylation sites (Leto *et al.*, 2012). There are two possibilities that ET-1-induced inhibition of insulin signaling results from (i) the interaction of IRS-1 with GRK2, or (ii) GRK2-mediated phosphorylation of IRS-1. In the present study, the interaction of IRS-1 with GRK2 was not detected by a coimmunoprecipitation assay in L6 myotubes overexpressing FLAG-GRK2 (Supplementary Figure S3). The possible involvement of GRK2-mediated IRS-1 phosphorylation in the ET-1-induced, GRK2-dependent insulin resistance will be studied in the future.

Conclusions

In summary, the present study has shown the mechanism for the ET-1-induced inhibition of insulin signaling (i.e., insulin resistance) in L6 myotubes, as summarized in Figure 10. In L6 myotubes, insulin stimulates the PI3K-dependent Akt phosphorylation, which facilitates glucose uptake by augmenting translocation of GLUT4 to the plasma membrane. Activation of ET_AR with ET-1 facilitates the interaction of GRK2 with Akt via G_q protein-dependent pathway. Overexpression of GRK2-ct counteracts ET-1-induced, GRK2-mediated inhibition of the insulin-stimulated Akt phosphorylation and glucose uptake. Thus, activation of ET_AR with ET-1 induces the insulin resistance by facilitating the interaction of GRK2 with Akt. These results indicate that both ET_AR and GRK2 are therapeutic targets for insulin resistance.

Acknowledgements

We thank Dr. Hitoshi Kurose (Kyusyu University, Japan) for kindly donating recombinant adenoviruses encoding GFP and GRK2-ct, and the pcDNA3 mammalian expression vector encoding FLAG-GRK2. We also thank Astellas Pharma Inc. (Tokyo, Japan) for the generously providing YM-254890.

Source of funding

This study was supported in part by Grants-in-Aid for Scientific Research (C) from Japan Society for the Promotion of Science [grant 24590309] (to T. Horinouchi), Grants-in-Aid for Scientific Research (B) from Japan Society for the Promotion of Science [grant 24390059] (to S.M.) and by grants from Smoking Research Foundation of Japan (to S.M.), the Pharmacological Research Foundation, Tokyo (to T. Horinouchi), Suzuken Memorial Foundation (to T. Horinouchi), and Actelion Pharmaceuticals Japan Ltd. (to T. Higa).

Conflict of interest

The authors state no conflict of interest.

References

Alexander SP, Mathie A, Peters JA (2011). Guide to Receptors and Channels (GRAC), 5th edition. *Br J Pharmacol* **164:** S1-S324.

Bentzinger CF, Wang YX, Rudnicki MA (2012). Building muscle: molecular regulation of myogenesis. *Cold Spring Harb Perspect Biol* **4:** ID a008342.

Bradford MM (1976). A rapid and sensitive method for the quantitation of microgram quantities of protein utilizing the principle of protein-dye binding. *Anal Biochem* **72:** 248-254.

DeFronzo RA (1988). Lilly lecture 1987. The triumvirate: beta-cell, muscle, liver. A collusion responsible for NIDDM. *Diabetes* **37:** 667-687.

Evron T, Daigle TL, Caron MG (2012). GRK2: multiple roles beyond G protein-coupled receptor desensitization. *Trends Pharmacol Sci* **33:** 154-164.

Ferri C, Bellini C, Desideri G, Di Francesco L, Baldoncini R, Santucci A, *et al.* (1995). Plasma endothelin-1 levels in obese hypertensive and normotensive men. *Diabetes* **44:** 431-436.

Gomes AR, Soares AG, Peviani S, Nascimento RB, Moriscot AS, Salvini TF (2006). The effect of 30 minutes of passive stretch of the rat soleus muscle on the myogenic differentiation, myostatin, and atrogin-1 gene expressions. *Arch Phys Med Rehabil* **87:** 241-246.

Harada T, Horinouchi T, Higa T, Hoshi A, Higashi T, Terada K, *et al.* (2014). Endothelin-1 activates extracellular signal-regulated kinases 1/2 via transactivation of platelet-derived growth factor receptor in rat L6 myoblasts. *Life Sci* **104:** 24-31.

Horinouchi T, Higashi T, Higa T, Terada K, Mai Y, Aoyagi H, *et al.* (2012). Different binding property of STIM1 and its novel splice variant STIM1L to Orai1, TRPC3, and TRPC6 channels. *Biochem Biophys Res Commun* **428:** 252-258.

Horinouchi T, Terada K, Higashi T, Miwa S (2013). Endothelin receptor signaling: new insight into its regulatory mechanisms. *J Pharmacol Sci* **123:** 85-101.

Imamura T, Vollenweider P, Egawa K, Clodi M, Ishibashi K, Nakashima N, *et al.* (1999). G alpha-q/11 protein plays a key role in insulin-induced glucose transport in 3T3-L1 adipocytes. *Mol Cell Biol* **19:** 6765-6774.

Jin P, Sejersen T, Ringertz NR (1991). Recombinant platelet-derived growth factor-BB stimulates growth and inhibits differentiation of rat L6 myoblasts. *J Biol Chem* **266:** 1245-1249.

Kamikawa Y, Ikeda S, Harada K, Ohwatashi A, Yoshida A (2013). Passive repetitive stretching for a short duration within a week increases myogenic regulatory factors and myosin heavy chain mRNA in rats' skeletal muscles. *ScientificWorldJournal* **2013:** ID 493656.

Kim I, Yang D, Tang X, Carroll JL (2011). Reference gene validation for qPCR in rat carotid body during postnatal development. *BMC Res Notes* **4:** ID 440.

Knight SD, Adams ND, Burgess JL, Chaudhari AM, Darcy MG, Donatelli CA, *et al.* (2010). Discovery of GSK2126458, a highly potent inhibitor of PI3K and the mammalian target of rapamycin. *ACS Med Chem Lett* **1:** 39-43.

Koch WJ, Hawes BE, Inglese J, Luttrell LM, Lefkowitz RJ (1994). Cellular expression of the

carboxyl terminus of a G protein-coupled receptor kinase attenuates $G_{\beta\gamma}$-mediated signaling. *J Biol Chem* **269:** 6193-6197.

Kurose H, Nishida M, Nagao T (1999). βγ subunit of heterotrimeric G protein as a new target molecule for drug development. *Folia Pharmacol Jpn* **114:** 75-80.

Laplante M, Sabatini DM (2012). mTOR signaling in growth control and disease. *Cell* **149:** 274-293.

Lerman A, Edwards BS, Hallett JW, Heublein DM, Sandberg SM, Burnett JCJ (1991). Circulating and tissue endothelin immunoreactivity in advanced atherosclerosis. *N Engl J Med* **325:** 997-1001.

Leto D, Saltiel AR (2012). Regulation of glucose transport by insulin: traffic control of GLUT4. *Nat Rev Mol Cell Biol* **13:** 383-396.

Liu S, Premont RT, Kontos CD, Zhu S, Rockey DC (2005). A crucial role for GRK2 in regulation of endothelial cell nitric oxide synthase function in portal hypertension. *Nat Med* **11:** 952-958.

Lteif A, Vaishnava P, Baron AD, Mather KJ (2007). Endothelin limits insulin action in obese/insulin-resistant humans. *Diabetes* **56:** 728-734.

Mitsumoto Y, Burdett E, Grant A, Klip A (1991). Differential expression of the GLUT1 and GLUT4 glucose transporters during differentiation of L6 muscle cells. *Biochem Biophys Res Commun* **175:** 652-659.

Mitsumoto Y, Klip A (1992). Development regulation of the subcellular distribution and glycosylation of GLUT1 and GLUT4 glucose transporters during myogenesis of L6 muscle

cells. *J Biol Chem* **267:** 4957-4962.

Nevzorova J, Bengtsson T, Evans BA, Summers RJ (2002). Characterization of the β-adrenoceptor subtype involved in mediation of glucose transport in L6 cells. *Br J Pharmacol* **137:** 9-18.

Nishida M, Maruyama Y, Tanaka R, Kontani K, Nagao T, Kurose H (2000). G α_i and G α_o are target proteins of reactive oxygen species. *Nature* **408:** 492-495.

Öberg A, Dehvari N, Bengtsson T (2011). β-Adrenergic inhibition of contractility in L6 skeletal muscle cells. *PLoS One* **6:** e22304.

Obici S, Feng Z, Karkanias G, Baskin DG, Rossetti L (2002). Decreasing hypothalamic insulin receptors causes hyperphagia and insulin resistance in rats. *Nat Neurosci* **5:** 566-572.

Ottosson-Seeberger A, Lundberg JM, Alvestrand A, Ahlborg G (1997). Exogenous endothelin-1 causes peripheral insulin resistance in healthy humans. *Acta Physiol Scand* **161:** 211-220.

Pernow J, Shemyakin A, Böhm F (2012). New perspectives on endothelin-1 in atherosclerosis and diabetes mellitus. *Life Sci* **91:** 507-516.

Rodríguez-Pascual F, Busnadiego O, Lagares D, Lamas S (2011). Role of endothelin in the cardiovascular system. *Pharmacol Res* **63:** 463-472.

Rubin LJ (2012). Endothelin receptor antagonists for the treatment of pulmonary artery hypertension. *Life Sci* **91:** 517-521.

Ruest LB, Marcotte R, Wang E (2002). Peptide elongation factor eEF1A-2/S1 expression in

cultured differentiated myotubes and its protective effect against caspase-3-mediated apoptosis. *J Biol Chem* **277:** 5418-5425.

Sarbassov DD, Guertin DA, Ali SM, Sabatini DM (2005). Phosphorylation and regulation of Akt/PKB by the rictor-mTOR complex. *Science* **307:** 1098-1101.

Schalin-Jäntti C, Yki-Järvinen H, Koranyi L, Bourey R, Lindström J, Nikula-Ijäs P, *et al.* (1994). Effect of insulin on GLUT-4 mRNA and protein concentrations in skeletal muscle of patients with NIDDM and their first-degree relatives. *Diabetologia* **37:** 401-407.

Shemyakin A, Salehzadeh F, Esteves Duque-Guimaraes D, Böhm F, Rullman E, Gustafsson T, *et al.* (2011). Endothelin-1 reduces glucose uptake in human skeletal muscle in vivo and in vitro. *Diabetes* **60:** 2061-2067.

Shepherd PR, Nave BT, Rincon J, Haigh RJ, Foulstone E, Proud C, *et al.* (1997). Involvement of phosphoinositide 3-kinase in insulin stimulation of MAP-kinase and phosphorylation of protein kinase-B in human skeletal muscle: implications for glucose metabolism. *Diabetologia* **40:** 1172-1177.

Shisheva A (2008). Phosphoinositides in insulin action on GLUT4 dynamics: not just PtdIns(3,4,5)P_3. *Am J Physiol Endocrinol Metab* **293:** E536-E544.

Takahashi K, Ghatei MA, Lam HC, O'Halloran DJ, Bloom SR (1990). Elevated plasma endothelin in patients with diabetes mellitus. *Diabetologia* **33:** 306-310.

Touyz RM, Schiffrin EL (2003). Role of endothelin in human hypertension. *Can J Physiol Pharmacol* **81:** 533-541.

Tsakiridis T, McDowell HE, Walker T, Downes CP, Hundal HS, Vranic M, *et al.* (1995).

Multiple roles of phosphatidylinositol 3-kinase in regulation of glucose transport, amino acid transport, and glucose transporters in L6 skeletal muscle cells. *Endocrinology* **136:** 4315-4322.

Usui I, Imamura T, Babendure JL, Satoh H, Lu JC, Hupfeld CJ, *et al.* (2005). G protein-coupled receptor kinase 2 mediates endothelin-1-induced insulin resistance via the inhibition of both Gαq/11 and insulin receptor substrate-1 pathways in 3T3-L1 adipocytes. *Mol Endocrinol* **19:** 2760-2768.

Usui I, Imamura T, Huang J, Satoh H, Olefsky JM (2003). Cdc42 is a Rho GTPase family member that can mediate insulin signaling to glucose transport in 3T3-L1 adipocytes. *J Biol Chem* **278:** 13765-13774.

Usui I, Imamura T, Satoh H, Huang J, Babendure JL, Hupfeld CJ, *et al.* (2004). GRK2 is an endogenous protein inhibitor of the insulin signaling pathway for glucose transport stimulation. *EMBO J* **23:** 2821-2829.

Yanagisawa M, Kurihara H, Kimura S, Tomobe Y, Kobayashi M, Mitsui Y, *et al.* (1988). A novel potent vasoconstrictor peptide produced by vascular endothelial cells. *Nature* **332:** 411-415.

Table 1. Oligonucleotides used as PCR primers

Gene	Forward Primer (5' to 3')	Reverse Primer (5' to 3')	Product size (bp)	References
Rat MyoD	GGAGACATCCTCAAGCGATGC	AGCACCTGGTAAATCGGATTG	105	(Gomes *et al.*, 2006)
Rat myogenin	ACTACCCACCGTCCATTCAC	TCGGGGCACTCACTGTCTCT	233	(Kamikawa *et al.*, 2013)
Rat 18S rRNA	CACGGGTGACGGGGAATCAG	CGGGTCGGGAGTGGGTAATTTG	105	(Kim *et al.*, 2011)
Rat ET_AR	ATGGGTGTCCTTTGCTTTCTGGCGT	TTAGTTCATGCTGTCCTTGTGGCTG	1,281	-
Rat G_q protein	ATGACTCTGGAGTCCATCATGGCGT	TTAGACCAGATTGTACTCCTTCAGG	1,080	-
Rat G_{11} protein	ATGACTCTGGAGTCCATGATAGCGT	TCAGACCAGGTTGTACTCCTTCAGG	1,080	-
Rat GRK2-ct	GCCAAAAACAAACAGCTGGGC	ACTGCCACGCTGAATCAGTGG	432	-
Rat IR	CAGGATTGGCGCTGTGTAAAC	CACAGCTGCCTCAGGTTCTG	491	(Obici *et al.*, 2002)
Rat Akt2	ATGAATGAGGTATCTGTCATCAAAG	TCACTCTCGGATGCTGGCTGAGTAG	1,446	-
Rat GLUT4	ATGCCGTCGGGTTTCCAGCAGATCGGC	TCAGTCATTCTCATCTGGCCCTAAGTATTC	1,530	-

Legends for figures

Figure 1.

Differentiation of L6 myoblasts into myotubes. (A) a protocol for differentiation of L6 myoblasts into myotubes. (B) phase contrast images of undifferentiated myoblasts (Day 0) and differentiated myotubes (Days 7 and 9) obtained at the same magnification. The nucleus was stained with Hoechst 33342 dye as shown in blue. (C and D) Changes in mRNA levels of differentiation marker gens, MyoD (C) and myogenin (D), during differentiation. Ordinate represents relative expression levels against 18S rRNA as an internal control gene. Data are presented as means ± S.E.M of the results obtained from 5 experiments.

Figure 2.

Characterization of Akt phosphorylation in response to insulin in L6 myotubes. (A) concentration-response curves for Akt phosphorylation in response to 5 min exposure to insulin with representative immunoblots using antibodies to phospho-Akt at Thr^{308} [p-Akt (T308)], phospho-Akt at Ser^{473} [p-Akt (S473)], and total Akt (t-Akt). (B) time course of Akt phosphorylation induced by 300 nM insulin with representative immunoblots. (C and D) effects of GSK2126458 and LY294002 on Akt phosphorylation in response to 5 min exposure to 300 nM insulin in L6 myotubes. The cells were treated with 10 nM GSK2126458 or 50 μM LY294002 for 30 min before stimulation with insulin. Representative immunoblots were obtained using antibodies to phospho-Akt at Thr^{308} [p-Akt (T308)], phospho-Akt at Ser^{473} [p-Akt (S473)], and total Akt (t-Akt). (A and B) Ordinate represents Akt phosphorylation responses which are normalized to the level of insulin-stimulated maximal Akt phosphorylation. (D) Ordinate represents Akt phosphorylation responses which are normalized to the level of insulin-stimulated Akt phosphorylation in L6 myotubes without treatment with GSK2126458 or LY294002. Data are presented as means ± S.E.M of the results obtained from 6 experiments. When no error bar is shown, the error is smaller than the symbol. $^{**}P < 0.01$, versus its control (300 nM insulin alone).

Figure 3.

Effect of ET-1 on Akt phosphorylation in response to 60 min exposure to 100 nM insulin in L6 myotubes. The cells were treated with 30 nM ET-1 for indicated times during treatment with 100 nM insulin for 60 min. Representative immunoblots were obtained using antibodies to phospho-Akt at Thr^{308} [p-Akt (T308)], phospho-Akt at Ser^{473} [p-Akt (S473)], and total Akt (t-Akt). Ordinate represents Akt phosphorylation responses which are normalized to the level of insulin-stimulated Akt phosphorylation in L6 myotubes without treatment with ET-1. Data are presented as means ± S.E.M of the results obtained from 5 - 6 experiments. When no error bar is shown, the error is smaller than the symbol.

Figure 4.

Effects of 0.1% DMSO (as a vehicle), BQ-123 (a selective ET_AR antagonist), BQ-788 (a selective ET_BR antagonist), YM-254890 (a selective G_q protein inhibitor), PTX (a selective G_i protein inhibitor), and NF449 (a G_s protein inhibitor) on the ET-1-induced inhibition of insulin-stimulated Akt phosphorylation in L6 myotubes. The cells were treated with 30 nM ET-1 for indicated times during treatment with 100 nM insulin for 60 min. The cells were treated with one of the drugs for 30 min (except PTX for 18 h) before treatment with 100 nM insulin for 60 min. (A) Representative immunoblots obtained using antibodies to phospho-Akt at Thr^{308} [p-Akt (T308)], phospho-Akt at Ser^{473} [p-Akt (S473)], and total Akt (t-Akt). (B) ET-1-induced changes in the ratio of phosphorylated Akt to total Akt. Ordinate represents Akt phosphorylation responses which are normalized to the level of insulin-stimulated Akt phosphorylation in L6 myotubes without treatment with ET-1, vehicle, antagonists, or inhibitors. Data are presented as means ± S.E.M of the results obtained from 5 - 6 experiments. $^{*}P < 0.05$, versus its control (100 nM insulin alone).

Figure 5.

Effects of introducing GFP (Adv-GFP) and GRK2-ct (Adv-GRK2-ct) by adenovirus infection on the ET-1-induced inhibition of insulin-stimulated Akt phosphorylation in L6 myotubes. The cells were treated with 30 nM ET-1 for indicated times during treatment with 100 nM

insulin for 60 min. (A) Representative immunoblots obtained using antibodies to phospho-Akt at Thr^{308} [p-Akt (T308)], phospho-Akt at Ser^{473} [p-Akt (S473)], total Akt (t-Akt), GFP and GRK2. Endogenously expressing GRK2 (Endo. GRK2) and exogenously expressing GRK2-ct (Exo. GRK2-ct) were detected with GRK 2 antibody (C-15) (Santa Cruz Biotechnology, Inc) which binds to the C-terminus of GRK 2. Arrow head indicates a nonspecific band in the lane of Exo. GRK2-ct. (B and C) ET-1-induced changes in the ratio of phosphorylated Akt to total Akt. Ordinate represents Akt phosphorylation responses which are normalized to the level of insulin-stimulated Akt phosphorylation in L6 myotubes without treatment with ET-1 and adenovirus. Data are presented as means ± S.E.M of the results obtained from 6 experiments. $^{*}P < 0.05$, versus its control (100 nM insulin alone). $^{\#}P < 0.05$, versus Adv-GFP-treated cells.

Figure 6.

Effects of introducing control and GRK2 siRNA on the ET-1-induced inhibition of insulin-stimulated Akt phosphorylation in L6 myotubes. The cells were treated with 30 nM ET-1 for indicated times during treatment with 100 nM insulin for 60 min. (A) Representative immunoblots obtained using antibodies to phospho-Akt at Thr^{308} [p-Akt (T308)], phospho-Akt at Ser^{473} [p-Akt (S473)], total Akt (t-Akt) and GRK2. (B and C) ET-1-induced changes in the ratio of phosphorylated Akt to total Akt. Ordinate represents Akt phosphorylation responses which are normalized to the level of insulin-stimulated Akt phosphorylation in L6 myotubes without treatment with ET-1 and siRNA. Data are presented as means ± S.E.M of the results obtained from 6 experiments. $^{*}P < 0.05$, versus its control (100 nM insulin alone). $^{\#}P < 0.05$, versus control siRNA-treated cells.

Figure 7.

Characterization of insulin-stimulated [^{3}H]2-DG uptake in L6 myotubes. (A) a protocol for [^{3}H]2-DG uptake assay. (B) Effects of GSK2126458 and LY294002 on insulin-stimulated [^{3}H]2-DG uptake. The cells were treated with the inhibitor for 30 min before stimulation with insulin. Ordinate represents the rate of [^{3}H]2-DG uptake (dpm μg^{-1} h^{-1}). (C)

concentration-response curves for insulin-stimulated [^{3}H]2-DG uptake in the absence and presence of 30 nM ET-1. Ordinate represents percentage of the rate of [^{3}H]2-DG uptake which is normalized to basal [^{3}H]2-DG uptake before application of insulin and ET-1. Data are presented as means ± S.E.M of the results obtained from 8 experiments. $^{*}P < 0.05$, $^{**}P < 0.01$, versus its control (insulin alone).

Figure 8.

Effects of BQ-123 (A), GRK2-ct overexpression (B) and GRK2 knockdown (C) on the ET-1-induced inhibition of insulin-stimulated [^{3}H]2-DG uptake in L6 myotubes. ET-1 was given concomitantly with insulin and [^{3}H]2-DG. Ordinate represents percentage of the rate of [^{3}H]2-DG uptake which is normalized to basal [^{3}H]2-DG uptake before application of insulin and ET-1. Data are presented as means ± S.E.M of the results obtained from 6 - 8 experiments. $^{*}P < 0.05$, between indicated columns.

Figure 9.

Interaction of endogenous Akt with FLAG-GRK2 in L6 myotubes. (A) Upper panel for immunoprecipitated samples (IP: α-normal IgG or FLAG): FLAG-tagged GRK2 proteins were immunoprecipitated with anti-FLAG antibody. Immunoprecipitates were probed with the anti-total Akt antibody to estimate coimmunoprecipitated endogenous Akt. Arrow head indicates a nonspecific band (lower band) for α-normal IgG in the lane of t-Akt. Lower panel for IP: FLAG-tagged GRK2 proteins were immunoprecipitated with anti-FLAG antibody, and the immunoprecipitates were probed with the anti-FLAG-HRP antibody to normalize the quantity of coimmunoprecipitated endogenous Akt. Upper panel for whole cell lysate (WCL): the expressed Akt was detected with the anti-total Akt antibody. Lower panel for WCL: the expressed FLAG-GRK2 was detected with the anti-FLAG-HRP antibody. (B and C) The histogram represents change in the ratio of the quantity of immunoprecipitated endogenous Akt to that of immunoprecipitated FLAG-GRK2. The change is normalized to the interaction of Akt with FLAG-GRK2 under resting conditions before application of insulin and ET-1. Data are presented as means ± S.E.M of the results obtained from 6

experiments. $^{*}P < 0.05$, versus basal interaction (in the absence of insulin and ET-1). $^{\#}P < 0.05$, between indicated columns.

Figure 10.

A schematic model showing the negative regulation of insulin signaling by ET-1 in L6 myotubes.

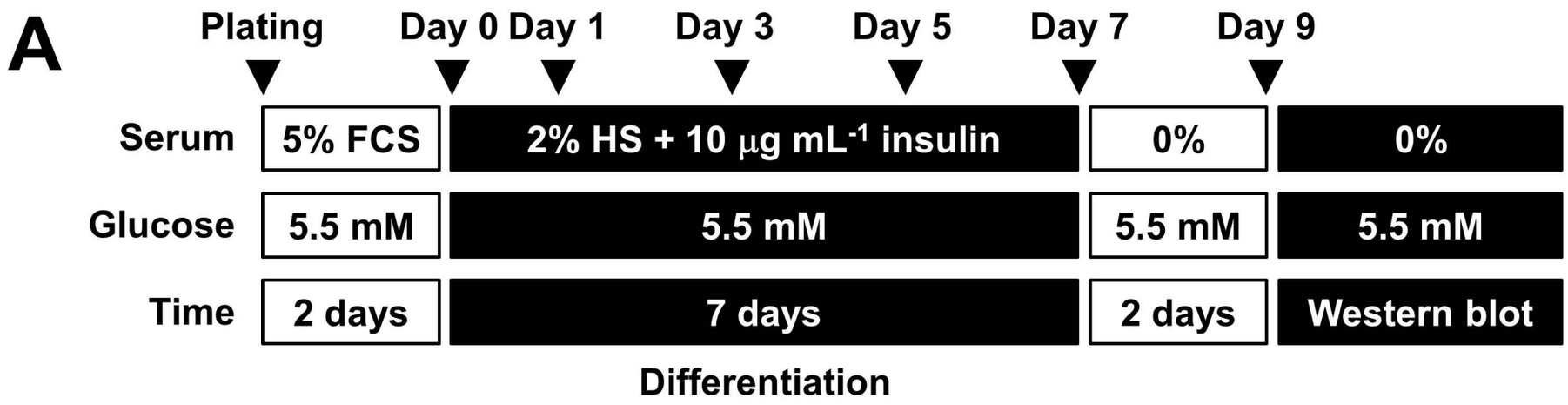
A
Plating
Day 0
Day 1
Day 3
Day 5
Day 7
Day 9
Serum
5% FCS
2% HS + 10 μg mL-1 insulin
0%
0%
Glucose
5.5 mM
5.5 mM
5.5 mM
5.5 mM
Time
2 days
7 days
2 days
Western blot
Differentiation

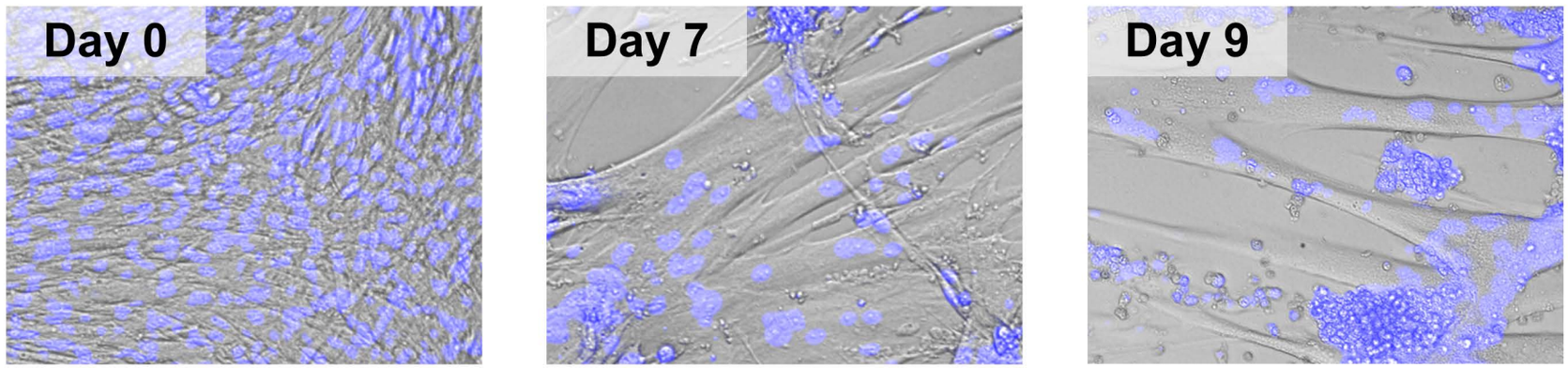
B
Day 0
Day 7
Day 9

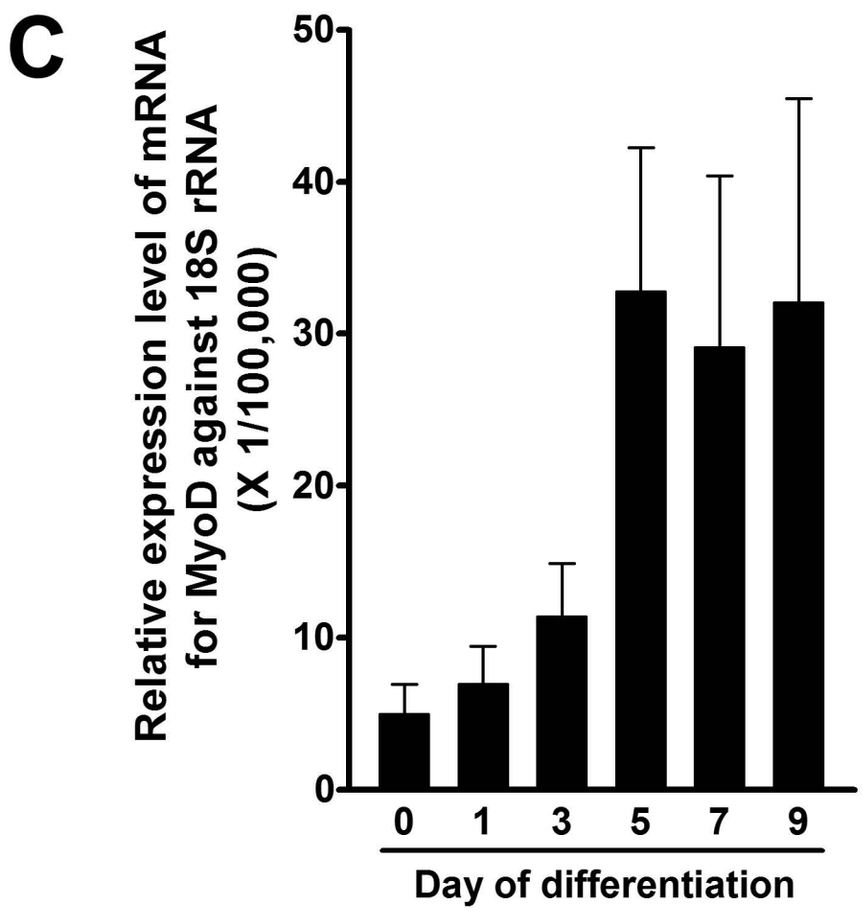
C
Relative expression level of mRNA for MyoD against 18S rRNA (X 1/100,000)
50
40
30
20
10
0
0
1
3
5
7
9
Day of differentiation

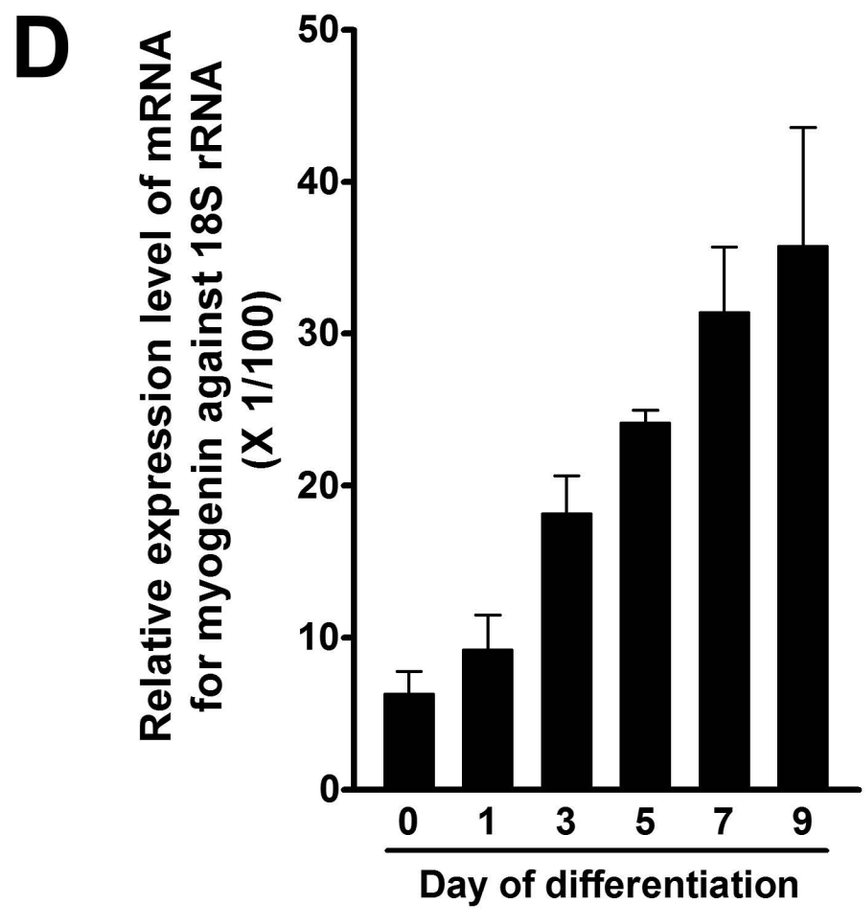
D
Relative expression level of mRNA for myogenin against 18S rRNA (X 1/100)
50
40
30
20
10
0
0
1
3
5
7
9
Day of differentiation

Figure 1

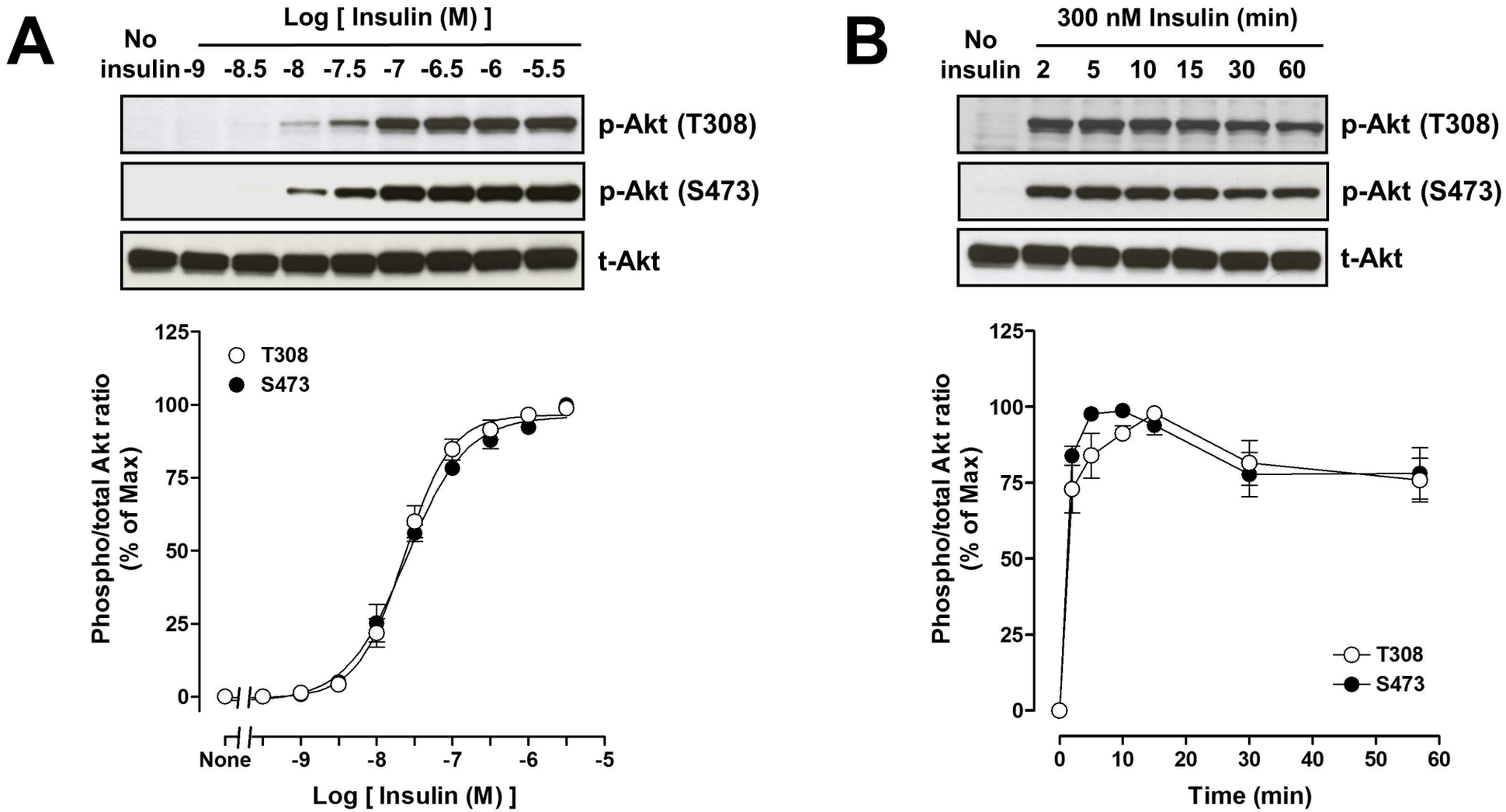
A
No insulin
Log [Insulin (M)]
-9 -8.5 -8 -7.5 -7 -6.5 -6 -5.5
p-Akt (T308)
p-Akt (S473)
t-Akt
Phospho/total Akt ratio (% of Max)
125
100
75
50
25
0
T308
S473
None -9 -8 -7 -6 -5
Log [Insulin (M)]
B
No insulin
300 nM Insulin (min)
2 5 10 15 30 60
p-Akt (T308)
p-Akt (S473)
t-Akt
Phospho/total Akt ratio (% of Max)
125
100
75
50
25
0
T308
S473
0 10 20 30 40 50 60
Time (min)

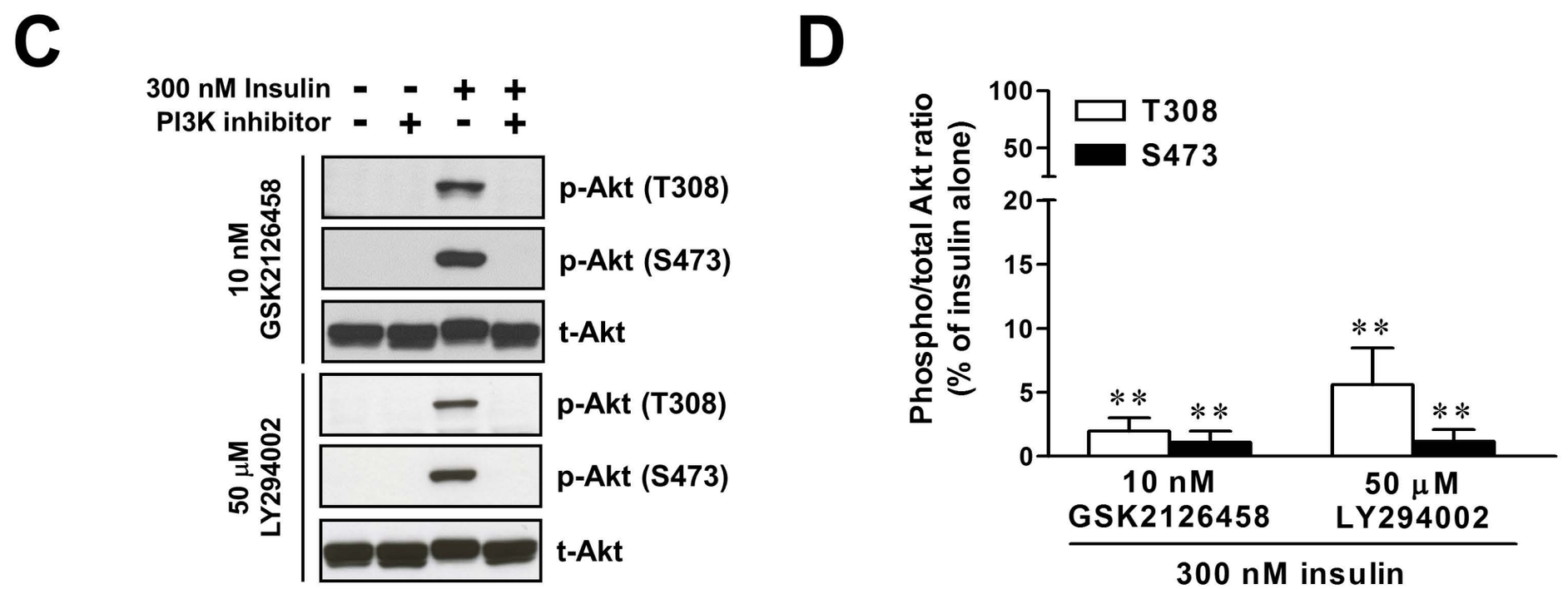
C
300 nM Insulin - - + +
PI3K inhibitor - + - +
10 nM GSK2126458
p-Akt (T308)
p-Akt (S473)
t-Akt
50 µM LY294002
p-Akt (T308)
p-Akt (S473)
t-Akt
D
Phospho/total Akt ratio (% of insulin alone)
100
50
20
15
10
5
0
T308
S473
**
**
**
**
10 nM GSK2126458
50 µM LY294002
300 nM insulin

Figure 2

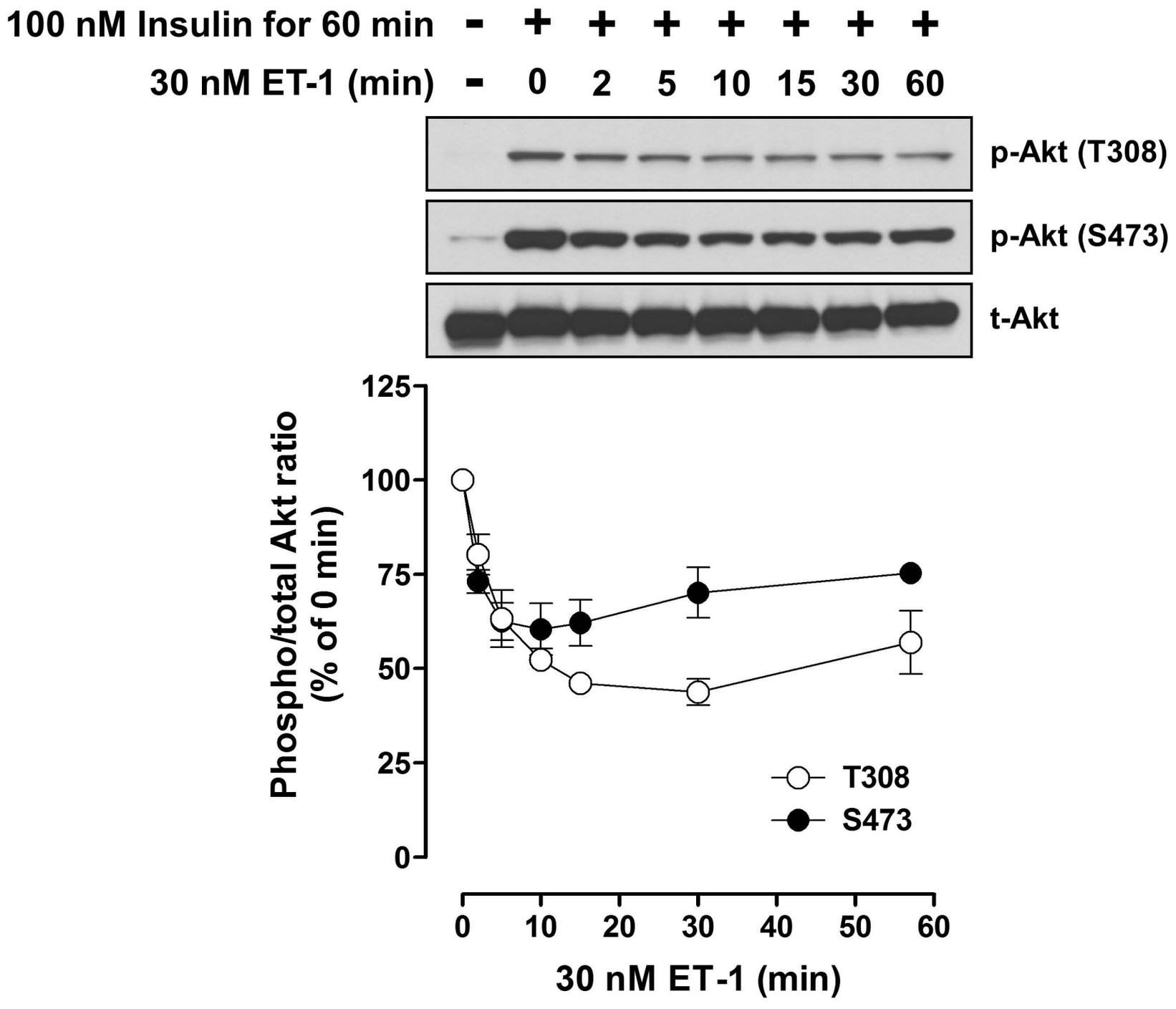
100 nM Insulin for 60 min - + + + + + + +
30 nM ET-1 (min) - 0 2 5 10 15 30 60
p-Akt (T308)
p-Akt (S473)
t-Akt
Phospho/total Akt ratio
(% of 0 min)
125
100
75
50
25
0
T308
S473
0 10 20 30 40 50 60
30 nM ET-1 (min)

Figure 3

A

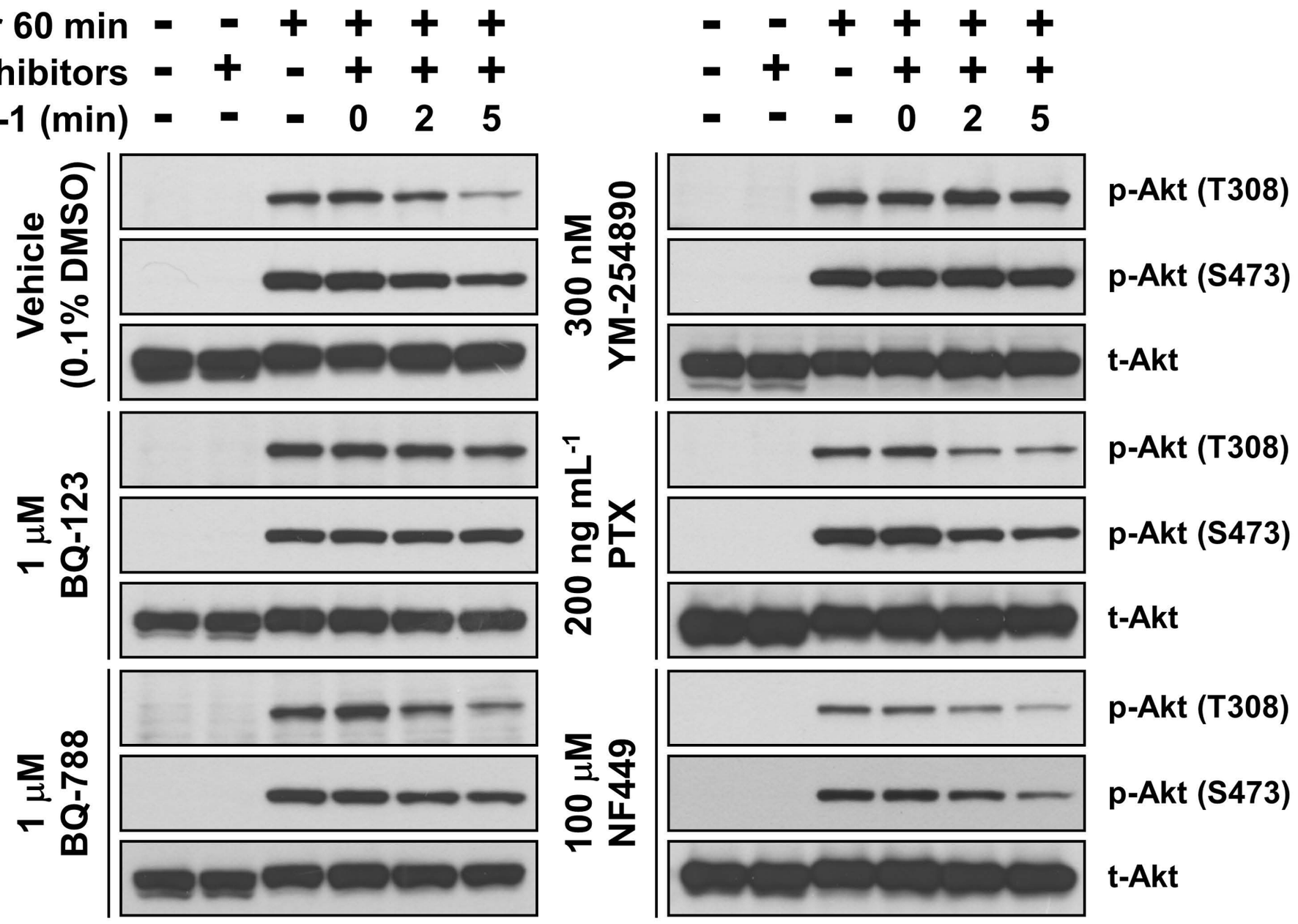
100 nM Insulin for 60 min - - + + + +
Antagonists or inhibitors - + - + + +
30 nM ET-1 (min) - - - 0 2 5
Vehicle (0.1% DMSO)
300 nM YM-254890
1 μM BQ-123
200 ng mL-1 PTX
1 μM BQ-788
100 μM NF449
p-Akt (T308)
p-Akt (S473)
t-Akt

B

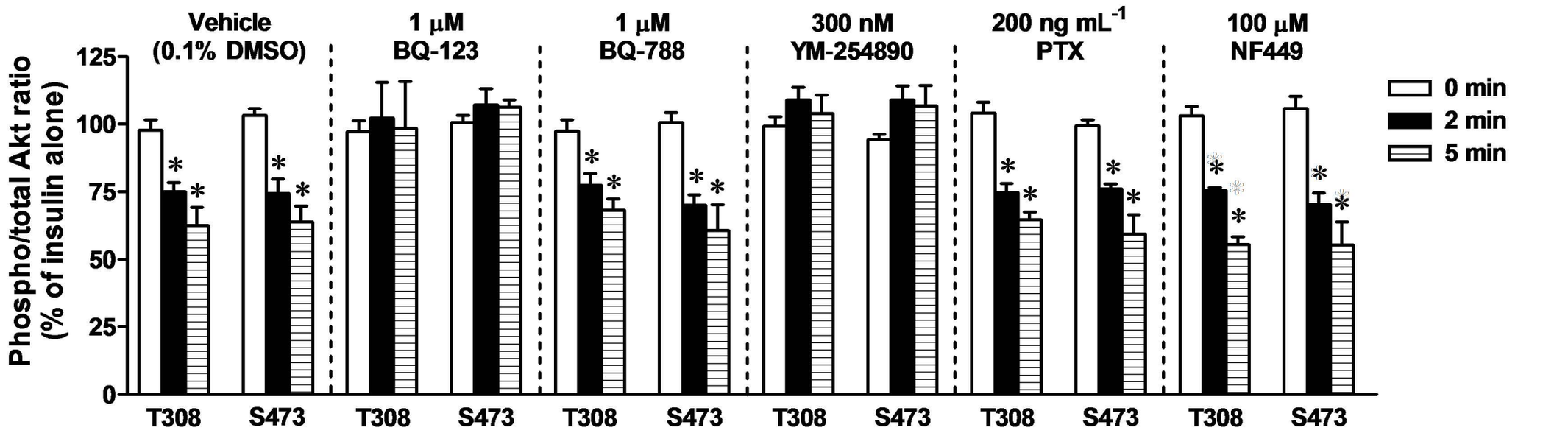
Phospho/total Akt ratio (% of insulin alone)
125
100
75
50
25
0
Vehicle (0.1% DMSO)
1 μM BQ-123
1 μM BQ-788
300 nM YM-254890
200 ng mL-1 PTX
100 μM NF449
T308
S473
0 min
2 min
5 min

Figure 4

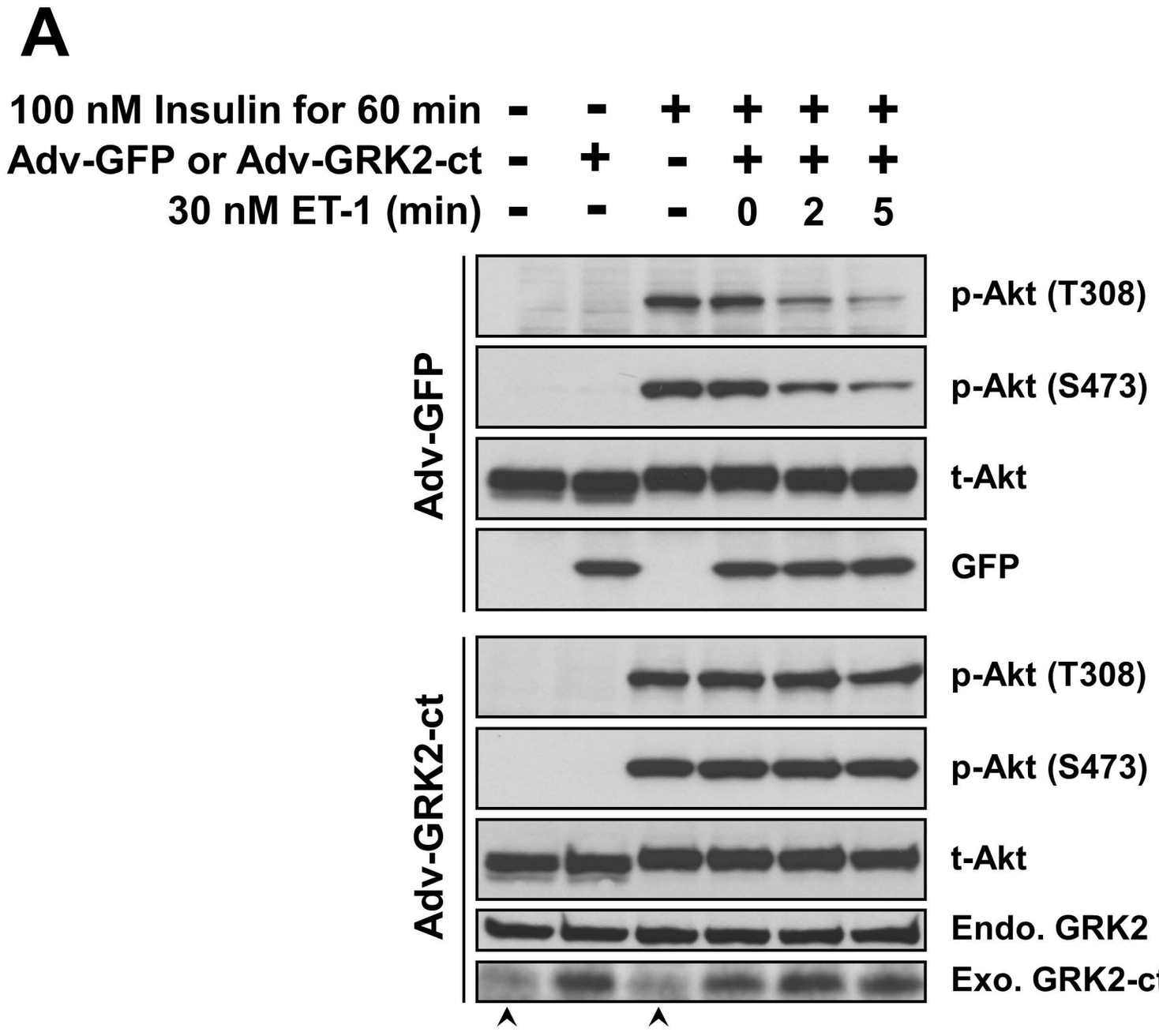
A
100 nM Insulin for 60 min - - + + + +
Adv-GFP or Adv-GRK2-ct - + - + + +
30 nM ET-1 (min) - - - 0 2 5
Adv-GFP
p-Akt (T308)
p-Akt (S473)
t-Akt
GFP
Adv-GRK2-ct
p-Akt (T308)
p-Akt (S473)
t-Akt
Endo. GRK2
Exo. GRK2-ct

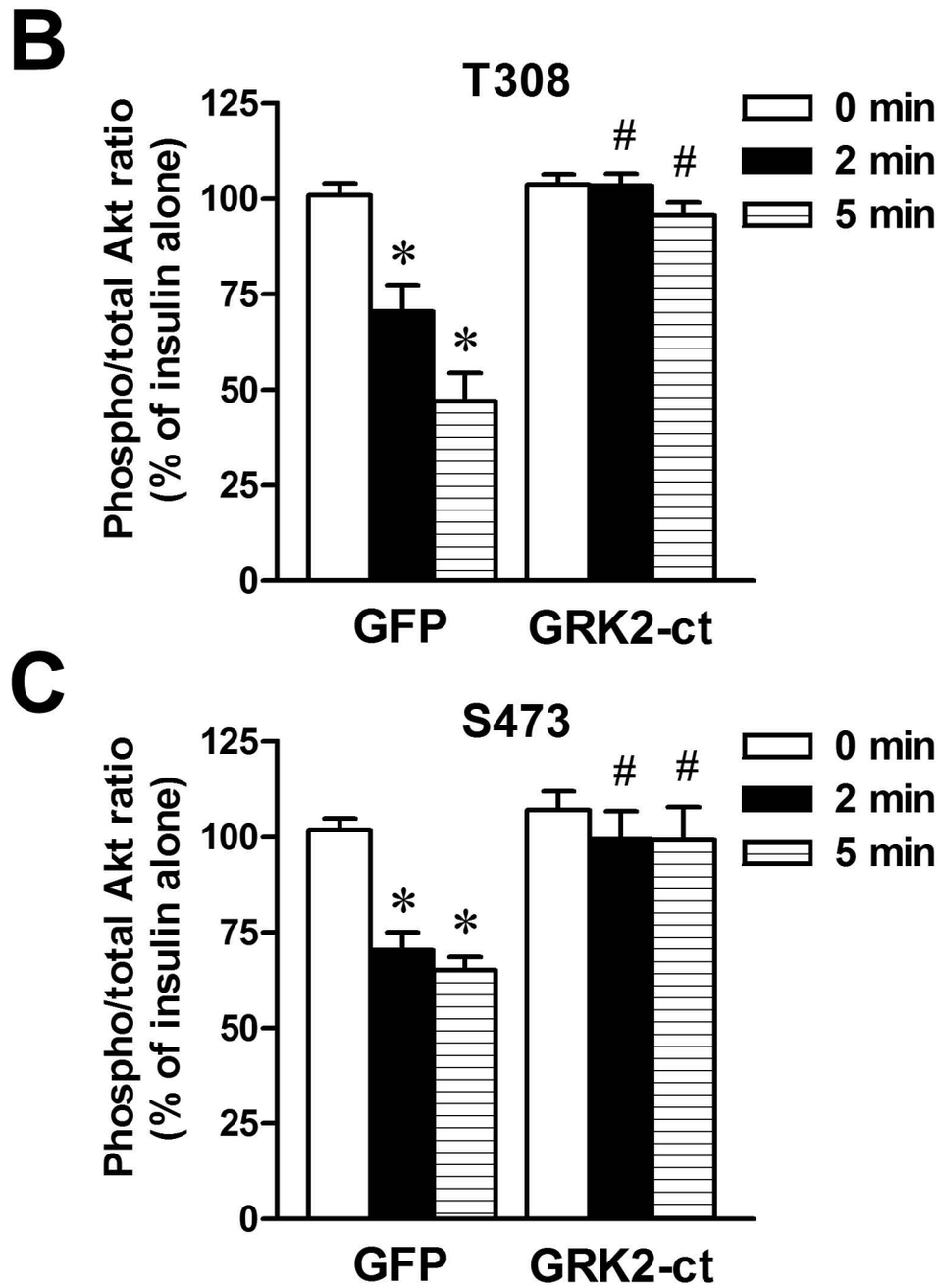
B
T308
Phospho/total Akt ratio (% of insulin alone)
125
100
75
50
25
0
0 min
2 min
5 min
*
*
#
#
GFP
GRK2-ct
C
S473
Phospho/total Akt ratio (% of insulin alone)
125
100
75
50
25
0
0 min
2 min
5 min
*
*
#
#
GFP
GRK2-ct

Figure 5

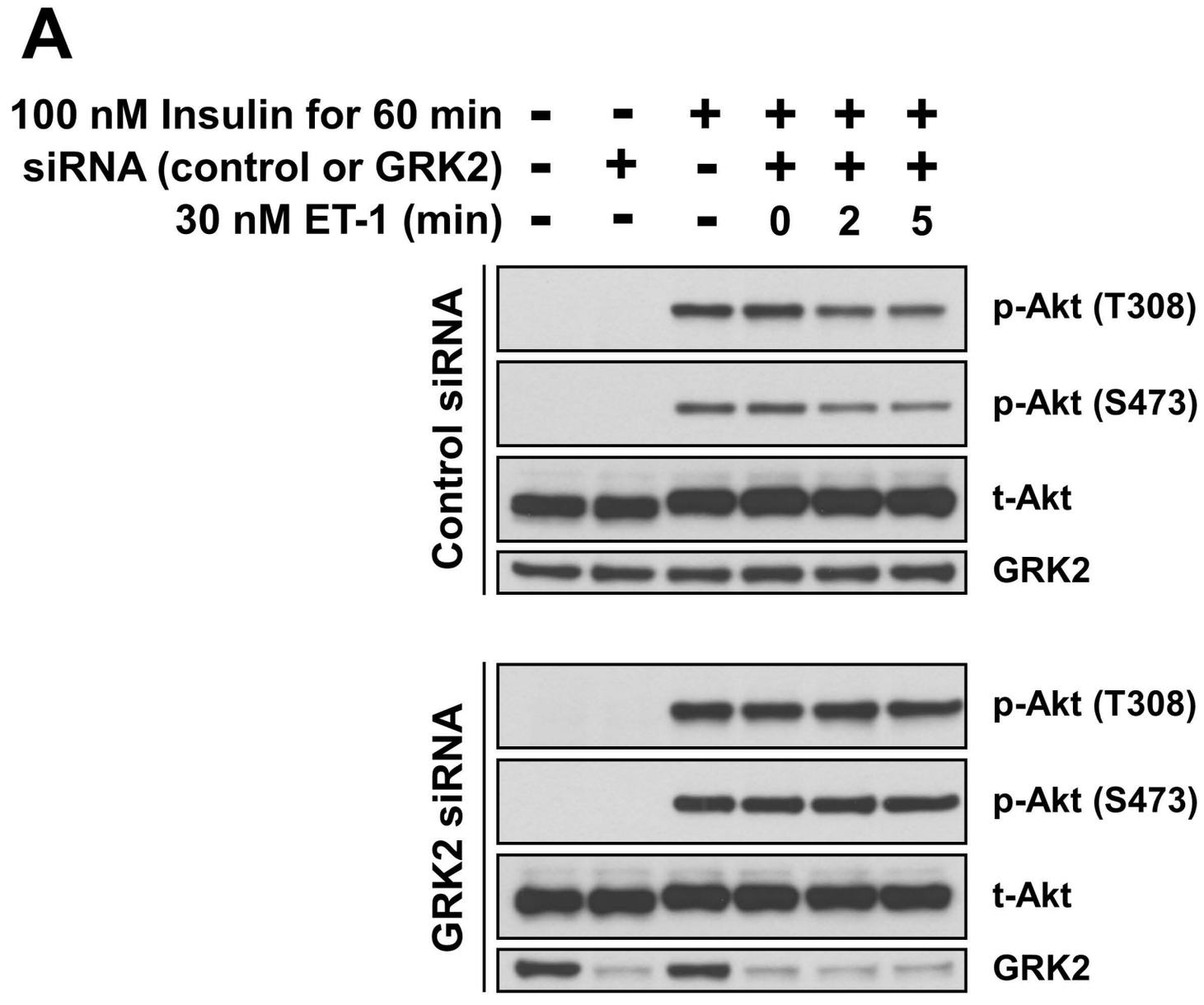
A
100 nM Insulin for 60 min - - + + + +
siRNA (control or GRK2) - + - + + +
30 nM ET-1 (min) - - - 0 2 5
Control siRNA
p-Akt (T308)
p-Akt (S473)
t-Akt
GRK2
GRK2 siRNA
p-Akt (T308)
p-Akt (S473)
t-Akt
GRK2

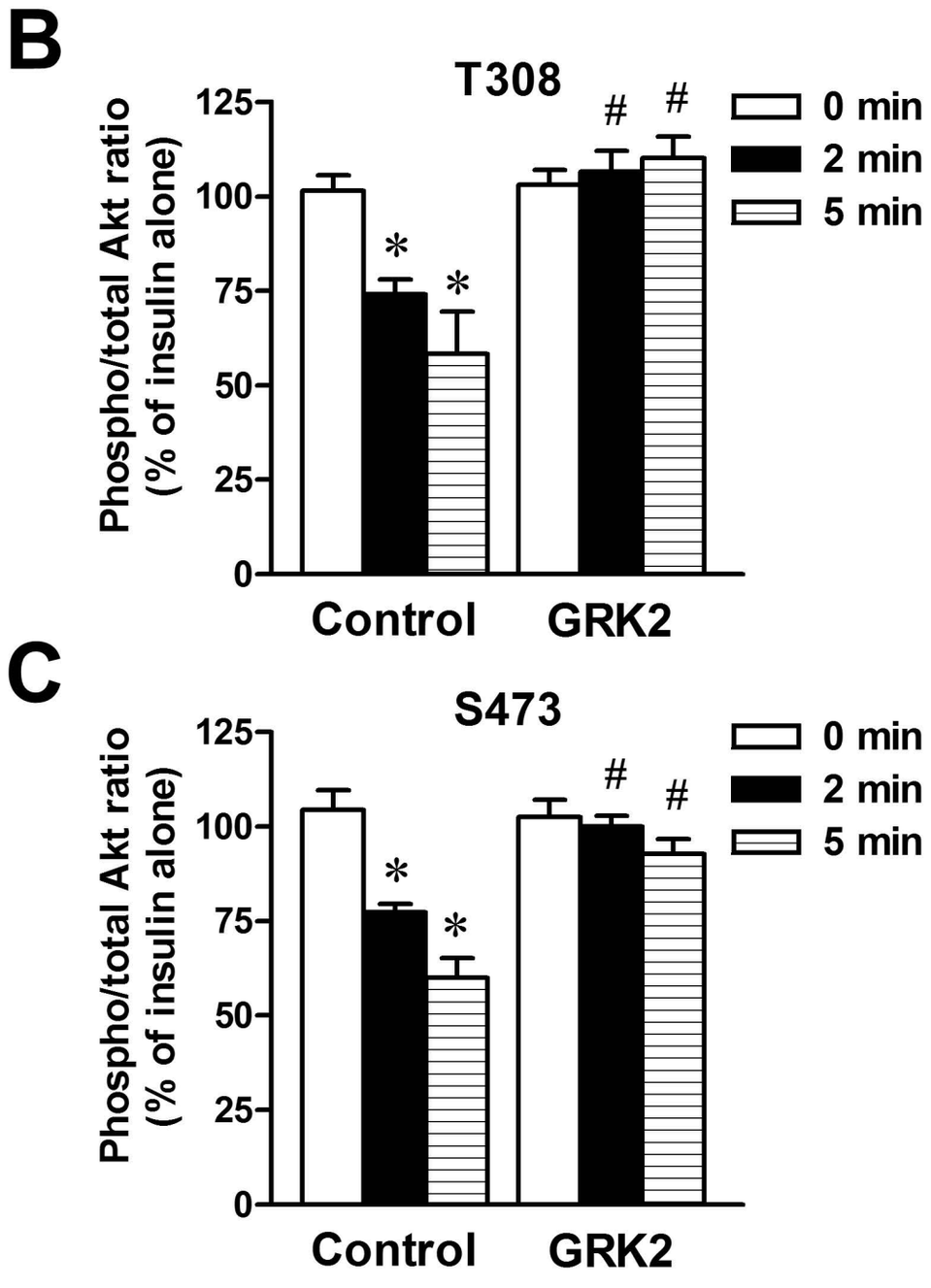
B
T308
Phospho/total Akt ratio (% of insulin alone)
125
100
75
50
25
0
*
*
#
#
0 min
2 min
5 min
Control
GRK2
C
S473
Phospho/total Akt ratio (% of insulin alone)
125
100
75
50
25
0
*
*
#
#
0 min
2 min
5 min
Control
GRK2

Figure 6

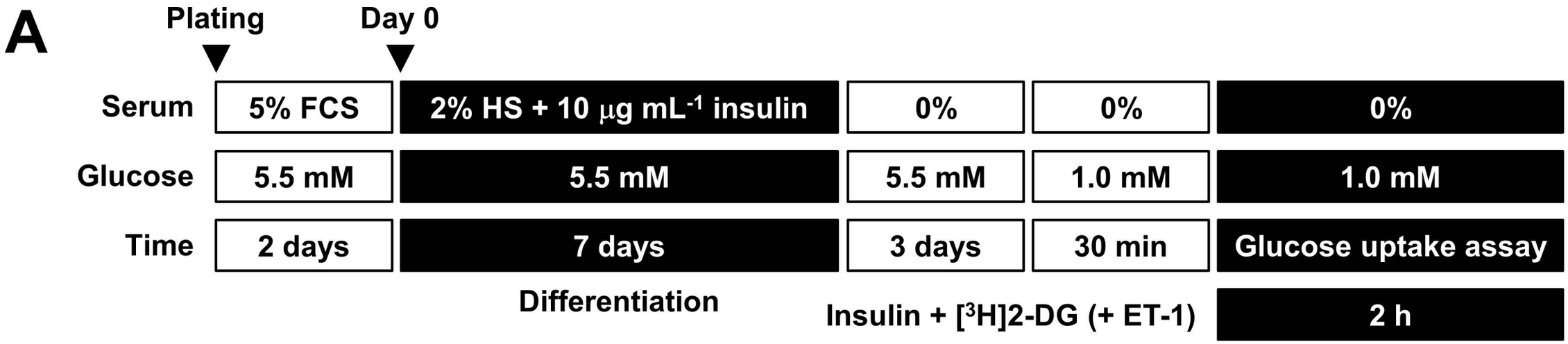
A
Plating
Day 0
Serum
5% FCS
2% HS + 10 μg mL-1 insulin
0%
0%
0%
Glucose
5.5 mM
5.5 mM
5.5 mM
1.0 mM
1.0 mM
Time
2 days
7 days
3 days
30 min
Glucose uptake assay
Differentiation
Insulin + [3H]2-DG (+ ET-1)
2 h

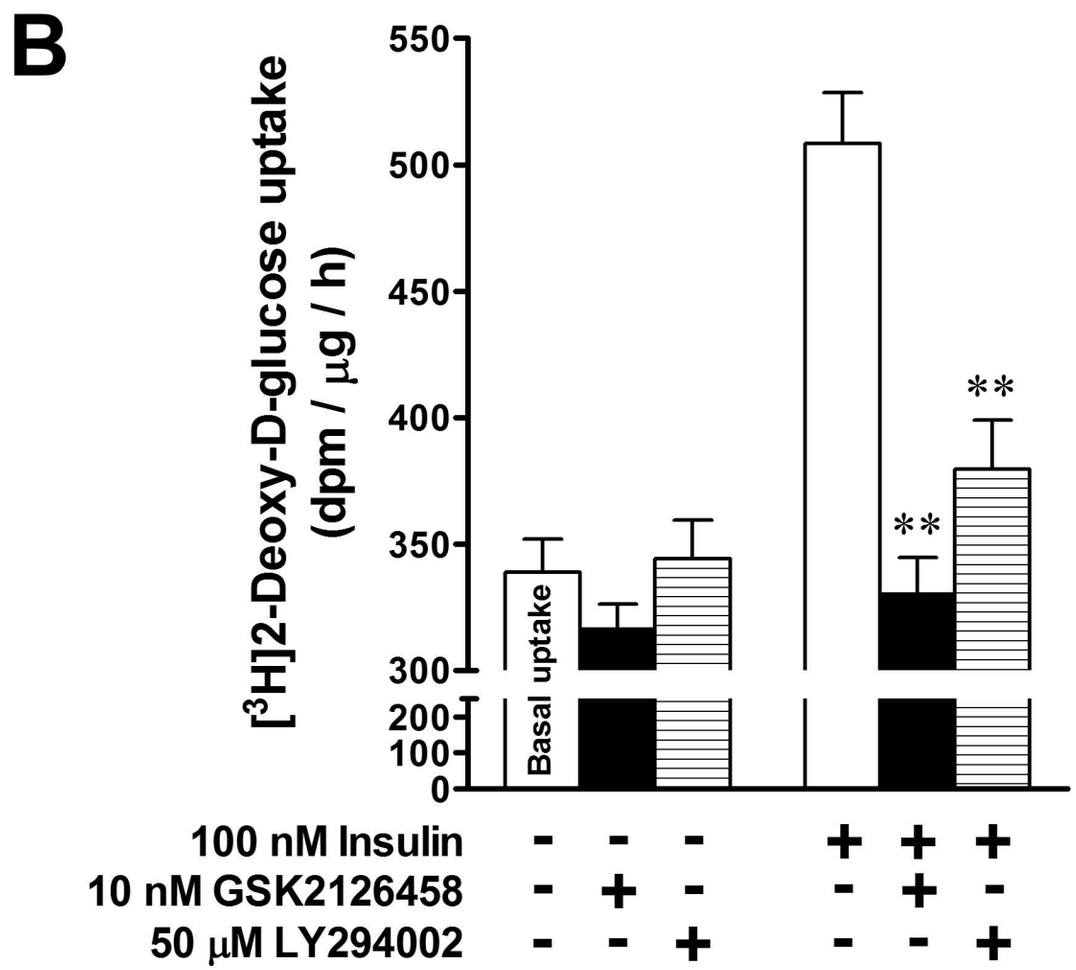
B
[3H]2-Deoxy-D-glucose uptake
(dpm / μg / h)
550
500
450
400
350
300
200
100
0
Basal uptake
**
**
100 nM Insulin - - - + + +
10 nM GSK2126458 - + - - + -
50 μM LY294002 - - + - - +

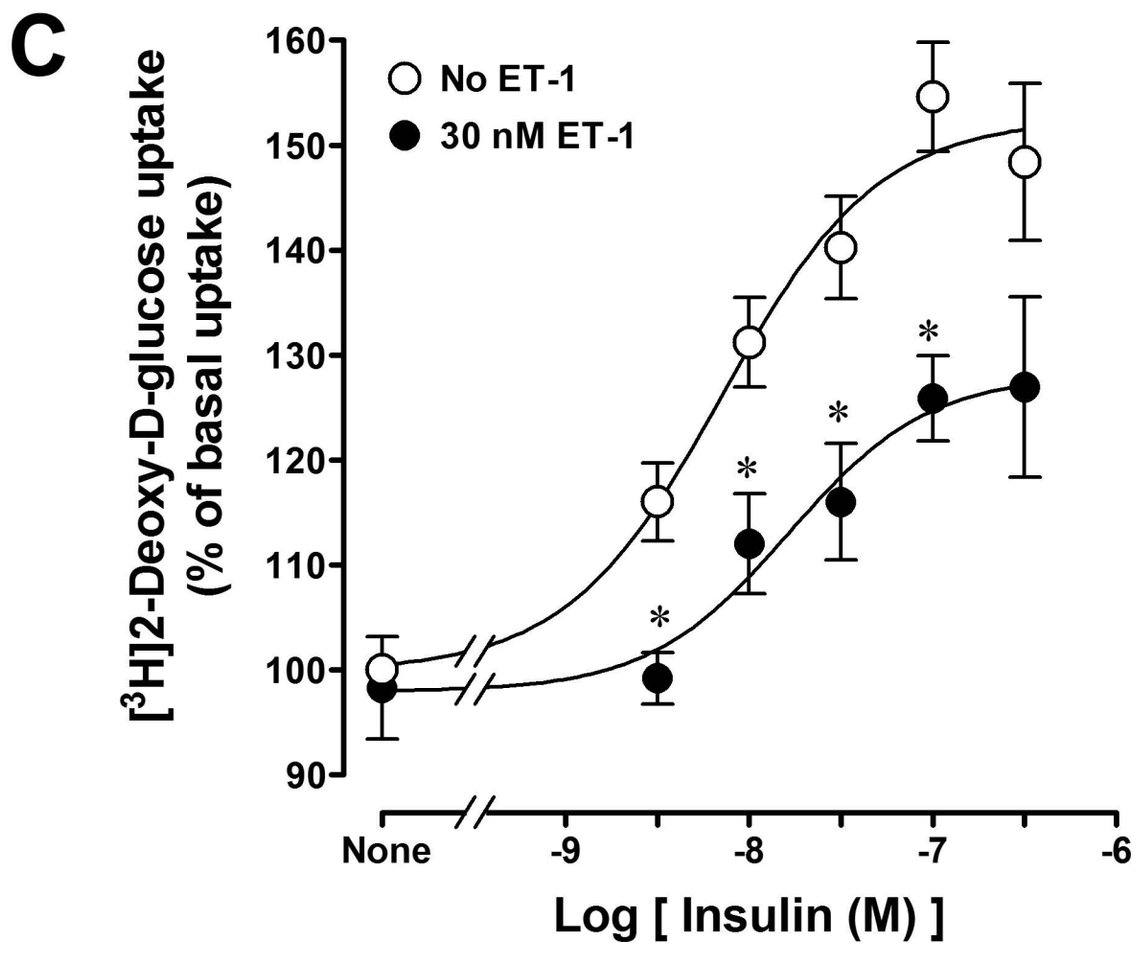
C
[3H]2-Deoxy-D-glucose uptake
(% of basal uptake)
160
150
140
130
120
110
100
90
No ET-1
30 nM ET-1
*
None
-9
-8
-7
-6
Log [Insulin (M)]

Figure 7

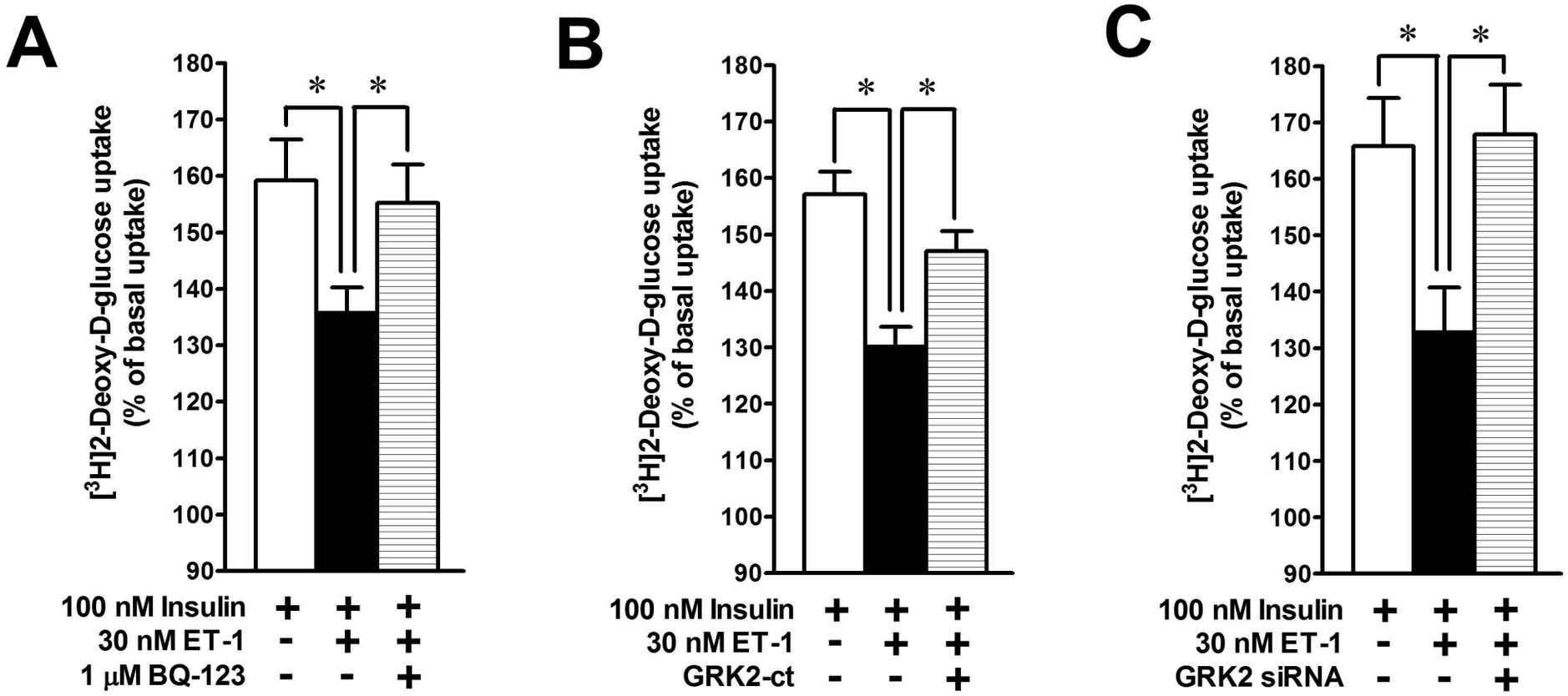
A
B
C
[3H]2-Deoxy-D-glucose uptake
(% of basal uptake)
180
170
160
150
140
130
120
110
100
90
*
*
100 nM Insulin + + +
30 nM ET-1 - + +
1 μM BQ-123 - - +
GRK2-ct - - +
GRK2 siRNA - - +

Figure 8

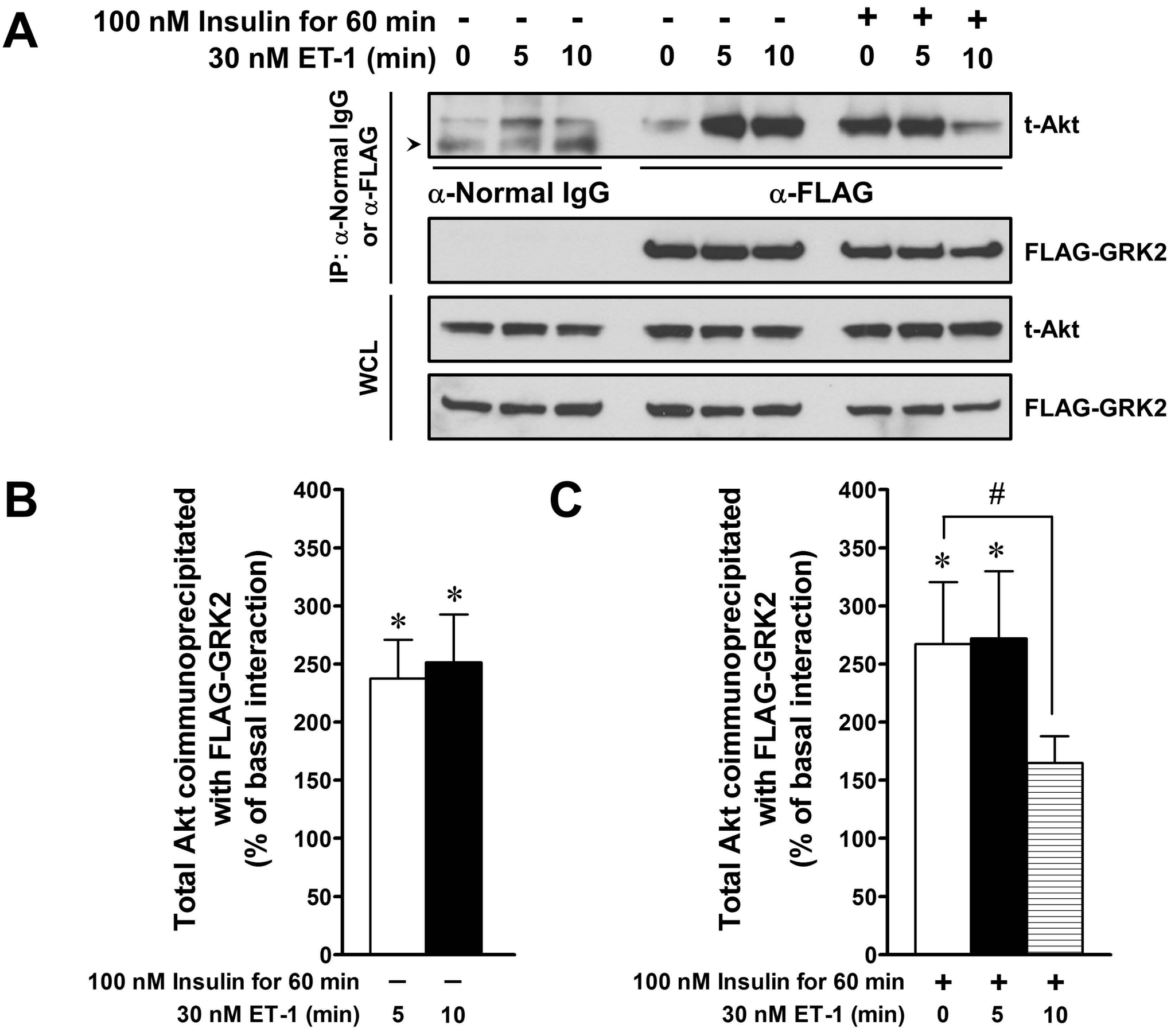
A
100 nM Insulin for 60 min - - - - - - + + +
30 nM ET-1 (min) 0 5 10 0 5 10 0 5 10
IP: α-Normal IgG or α-FLAG
WCL
t-Akt
α-Normal IgG
α-FLAG
FLAG-GRK2
t-Akt
FLAG-GRK2
B
Total Akt coimmunoprecipitated with FLAG-GRK2 (% of basal interaction)
400
350
300
250
200
150
100
50
0
*
*
100 nM Insulin for 60 min – –
30 nM ET-1 (min) 5 10
C
Total Akt coimmunoprecipitated with FLAG-GRK2 (% of basal interaction)
400
350
300
250
200
150
100
50
0
*
*
#
100 nM Insulin for 60 min + + +
30 nM ET-1 (min) 0 5 10

Figure 9

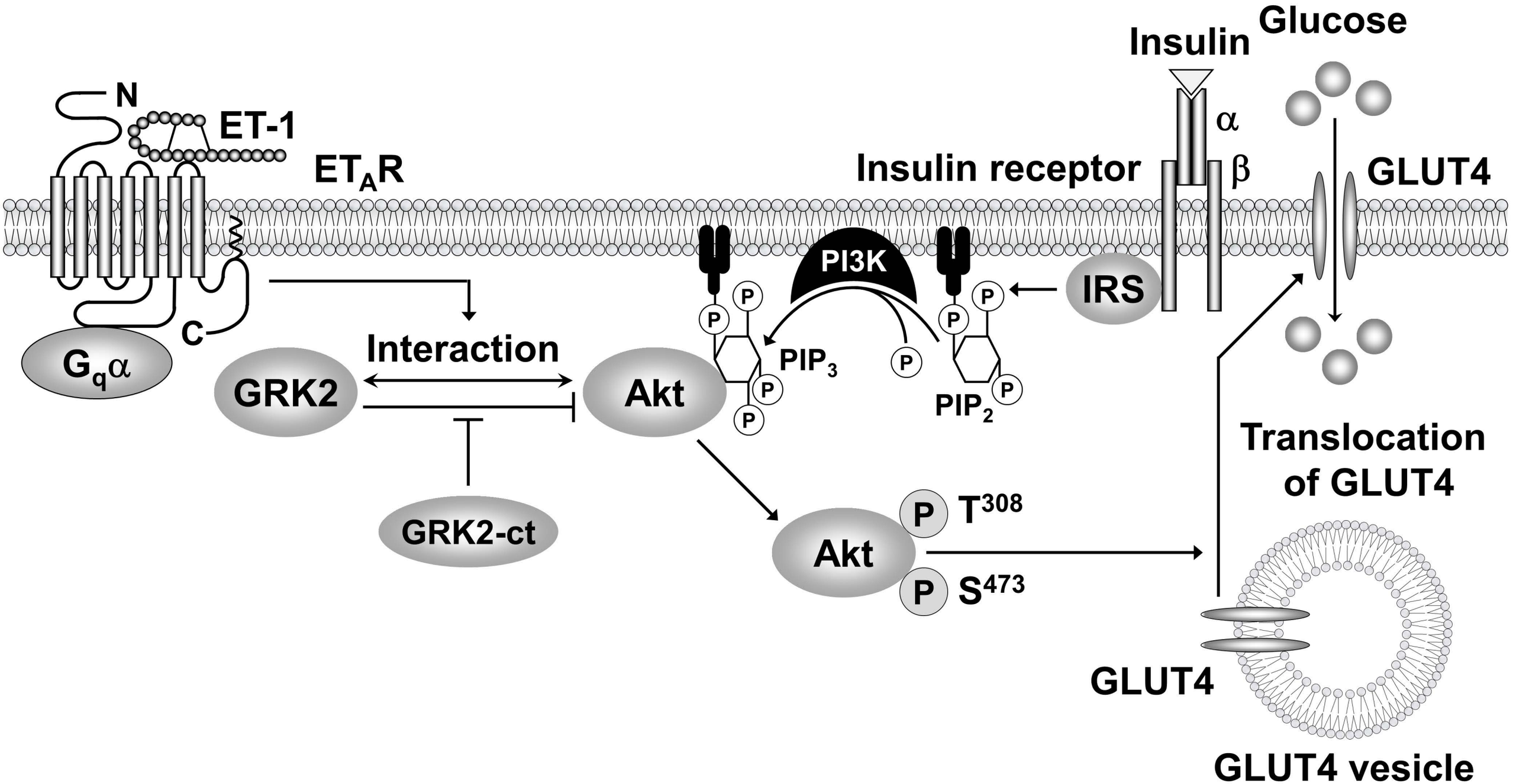
N
ET-1
ET_AR
$G_q\alpha$
C
GRK2
Interaction
GRK2-ct
Akt
PI3K
P
PIP_3
PIP_2
IRS
Insulin
Glucose
Insulin receptor
α
β
GLUT4
Translocation
of GLUT4
P T^{308}
Akt
P S^{473}
GLUT4
GLUT4 vesicle

Figure 10